

**ON THE DAMPED EULER–MONGE–AMPÈRE EQUATIONS WITH
RADIAL SYMMETRY:
CRITICAL THRESHOLDS AND LARGE-TIME BEHAVIOR**

KUNHUI LUAN

ABSTRACT. We investigate the global well-posedness and large-time dynamics of the pressureless Euler–Monge–Ampère (EMA) system with velocity damping in multidimensions, subject to radially symmetric initial data. We first establish the phenomenon of critical thresholds, where subcritical initial data maintain global regularity, and supercritical initial data lead to finite time singularity formation. We provide two methods for constructing these thresholds: a refined spectral dynamics approach based on [24] and a comparison principle based on Lyapunov functions introduced in [3].

A key finding of this work is that the inclusion of linear damping effectively removes the initial density lower bound previously required in the undamped case [31] in certain regimes, allowing for global regularity even in the presence of vacuum or arbitrarily low density. Furthermore, for subcritical initial data, we prove an optimal exponential decay rate to the equilibrium state. Our results unify and extend existing theories for 1D Euler–Poisson system and undamped multidimensional EMA system with radial symmetry.

CONTENTS

1. Introduction	2
1.1. Comparison with the Euler–Poisson system.	2
1.2. Outline of the paper.	4
2. Background and statement of main results.	4
2.1. Eulerian dynamics and the spectral dynamics	4
2.2. Local well-posedness	7
2.3. Global regularity versus finite time blowup	7
2.4. Large-time behavior	8
3. The damped Euler–Monge–Ampère system with radial symmetry.	8
3.1. Spectral dynamics for the radial damped Euler–Monge–Ampère system.	10
4. Proof of the main results.	13
4.1. A vacuous critical threshold	13
4.2. A non-vacuous critical threshold.	15

2020 *Mathematics Subject Classification.* 35B30, 35B40, 35B51, 35Q35, 35L67.

Key words and phrases. Euler–Monge–Ampère system, radial symmetry, multidimension, critical thresholds, Lyapunov functions, Euler–Poisson equation, well-posedness.

Acknowledgment. The author expresses sincere gratitude to Changhui Tan, Siming He, Qiyu Wu, Jesse Singh and Kyle Liss for numerous productive discussions and insightful feedback throughout the development of this work. This work has been partially supported by the NSF grant DMS-2238219 and the George Johnson Fellowships.

4.3. Explicit phase plane analysis.	16
4.4. Large-time behavior.	22
5. A Lyapunov function based approach to critical thresholds	24
Appendix A. Local well-posedness and regularity criterion	31
References	33

1. INTRODUCTION

We study the following pressureless compressible Euler equation with two forces

$$(1.1a) \quad \partial_t \rho + \nabla \cdot (\rho \mathbf{u}) = 0,$$

$$(1.1b) \quad \partial_t (\rho \mathbf{u}) + \nabla \cdot (\rho \mathbf{u} \otimes \mathbf{u}) = -\kappa \rho \nabla \phi - \beta \rho \mathbf{u},$$

$$(1.1c) \quad \det(\mathbb{I} - D^2 \phi) = \rho,$$

subject to initial data

$$(1.2) \quad \rho(\mathbf{x}, t=0) = \rho_0(\mathbf{x}), \quad \mathbf{u}(\mathbf{x}, t=0) = \mathbf{u}_0(\mathbf{x}), \quad \phi(\mathbf{x}, t=0) = \phi_0(\mathbf{x}).$$

Here $\rho(\cdot, t) : \mathbb{R}^n \mapsto \mathbb{R}_+$, $\mathbf{u}(\cdot, t) : \mathbb{R}^n \mapsto \mathbb{R}^n$ and $\phi(\cdot, t) : \mathbb{R}^n \mapsto \mathbb{R}$ denote the density, velocity and potential, respectively. Without loss of generality, we fix the potential assuming $\phi(0) = 0$.

The system is known as the damped *Euler–Monge–Ampère* (EMA) system. The right-hand side of the momentum equation (1.1b) includes two types of interacting forces: the *attractive-repulsive force* modeled by the Monge–Ampère equation and a *velocity damping*. Both constants κ and β are taken to be positive, with the former representing a repulsive force and the latter characterizing the damping strength.

The EMA system was first introduced in a discrete version by Y. Brenier in [5], with a subsequent kinetic counterpart, the Vlasov–Monge–Ampère system, proposed and analyzed in [7]. The development of the EMA system is fundamentally linked to the geometric framework established by V. Arnold in [1], who characterized the incompressible Euler equations on a fixed domain Ω as the geodesics of the right-invariant metric on the volume-preserving diffeomorphism group $\mathcal{D}_\mu(\Omega)$, based on the Lagrangian representation of fluid flows. Building on this, G. Loeper [25] formally introduced the EMA system as a geometric approximation to the incompressible Euler equations, specifically by approximating the geodesics on $\mathcal{D}_\mu(\Omega)$.

1.1. Comparison with the Euler–Poisson system. In addition to the EMA system, G. Loeper considered the following classical Euler–Poisson (EP) system in the same work [25],

$$(1.3a) \quad \partial_t \rho + \nabla \cdot (\rho \mathbf{u}) = 0,$$

$$(1.3b) \quad \partial_t (\rho \mathbf{u}) + \nabla \cdot (\rho \mathbf{u} \otimes \mathbf{u}) = -\kappa \rho \nabla \phi,$$

$$(1.3c) \quad -\Delta \phi = \rho - 1.$$

It was shown that both systems are asymptotically close and converge to the incompressible Euler equations in the quasi-neutral limit. Specifically, the EMA system can be viewed as a nonlinear generalization of the EP system. Indeed, we consider a perturbation near the equilibrium state $(\rho, \mathbf{u}) = (1, \mathbf{0})$, where the Monge–Ampère equation linearizes to the Poisson equation,

$$\rho = \det(I - \varepsilon D^2 \phi) = 1 - \varepsilon \Delta \phi + \mathcal{O}(\varepsilon^2).$$

The Euler–Poisson system models various physical phenomena, including semiconductor and plasma dynamics. The stability of the Euler–Poisson system near the equilibrium state was analyzed in [17, 19, 21, 18, 15]. Notably, in the one-dimensional case, the Monge–Ampère equation (1.1c) reduces to the Poisson equation $-\partial_{xx}\phi = \rho - 1$, rendering the EMA and EP systems equivalent. The global well-posedness theory for the 1D pressureless Euler–Poisson system with a constant background charge was first established in [14]. The global behavior of the solution exhibits a *critical threshold* phenomenon—specifically, a dichotomy in the initial data: *subcritical data* lead to global smooth solutions, while *supercritical data* result in finite-time singularity formation (see Theorem 2.2 for precise definitions). Furthermore, [14] provides an explicit and sharp expression for this threshold.

A generalization of the Euler–Poisson system arises when the background charge is not constant. The critical threshold phenomenon for this system has been recently investigated in [2, 12, 28, 26]. In particular, [12] establishes subcritical and supercritical regions under the presence of additional velocity damping, which was further extended in [26] to a nonlocal velocity alignment term. A series of *comparison principles* were developed based on Lyapunov functions introduced in [3], leading to the identification of non-trivial subcritical and supercritical regions, which underlies one of the main approach in this paper.

Several works have explored weak solutions to the Euler–Poisson system, particularly in 1D [16, 27, 6, 10]. The system has also been studied with the inclusion of pressure [17, 32, 19, 15]. Global theory for smooth solutions is known for radially symmetric data [34, 33, 11, 22]. For general data, critical thresholds are established for a 2D restricted Euler–Poisson (REP) system in [30, 24], but the system in two or three dimensions are less understood, and global regularity for the Euler–Poisson system remains an open question.

The close relationship between the EMA and EP systems naturally raises the question of whether a critical threshold phenomenon exists for the EMA system. An affirmative answer was first provided by E. Tadmor and C. Tan in [31], who presented a comprehensive analysis on the global regularity of EMA system with radial symmetry. They established a sharp and explicit critical threshold phenomenon. A salient feature of their result, however, is that global regularity in n dimensions necessitates a lower bound on the initial density, specifically $\rho_0 \geq 2^{-n}$ (See [31, Remark 3.5]). In particular, the system necessarily experiences a vacuous blow up.

Building on the work of Tadmor and Tan [31], this paper investigates the global regularity and large-time dynamics of the EMA system under radial symmetry with the inclusion of velocity damping. Our primary contribution is two-fold: we first derive *sharp* and *explicit* critical thresholds in Theorem 4.2, 4.1 and 5.4, and second, we establish an optimal uniform-in-time exponential decay rate of the solution toward the equilibrium state $(\rho, \mathbf{u}) = (1, \mathbf{0})$ in Theorem 4.3. We demonstrate that the introduction of damping effectively removes the initial density lower bound required in [31] in certain regimes. Specifically, we show that under *strong* and *critical* damping regimes, global regularity can be preserved even in the presence of vacuum or arbitrarily low initial density; see Remark 4.2.

We establish the threshold conditions through two complementary frameworks: first, by utilizing the spectral dynamics introduced in [24] through a refined phase plane analysis; and second, via a comparison principle based on Lyapunov functions. Furthermore, leveraging the explicit phase plane analysis, we characterize the large-time asymptotic behavior of the system. Our results serve as a unifying framework: in the one-dimensional case, we recover the damped Euler–Poisson thresholds obtained in [3], while in the absence of damping, we retrieve the results of [31].

1.2. Outline of the paper. The remainder of this paper is organized as follows. In Section 2, we briefly review Eulerian dynamics with radial symmetry, following the general framework established in [33], and present our main results for the damped EMA system. In Section 3, we derive the spectral dynamics governing the system. These dynamics are then utilized in Section 4 to construct the critical thresholds and analyze the large-time asymptotic behavior. This section also provides a detailed characterization of the critical thresholds for both vacuous and non-vacuous initial data. In Section 5, we present an alternative construction of the threshold regions using Lyapunov functions. Finally, an energy estimate proof of the local well-posedness result is provided in Appendix A.

2. BACKGROUND AND STATEMENT OF MAIN RESULTS.

In this paper, we focus on the class of no-swirl, radially symmetric solution of the form

$$(2.1) \quad \rho(\mathbf{x}, t) = \rho(|\mathbf{x}|, t), \quad \mathbf{u}(\mathbf{x}, t) = \frac{\mathbf{x}}{|\mathbf{x}|} u(|\mathbf{x}|, t), \quad \phi(\mathbf{x}, t) = \phi(|\mathbf{x}|, t), \quad r = |\mathbf{x}|.$$

We denote the radial variable by r , and ρ , u and ϕ are scalar functions defined in $\mathbb{R}_+ \times \mathbb{R}_+$. In addition, to ensure regularity of \mathbf{u} and ρ at the origin, we impose the following boundary conditions at $r = 0$

$$(2.2) \quad \partial_r \rho(0, t) = 0, \quad u(0, t) = 0, \quad \partial_r \phi(0, t) = 0.$$

We also restrict our attention to the case where

$$(2.3) \quad \phi_0''(r) \leq 1.$$

In particular, this assumption implies, in combination with (2.2), that $\frac{\phi_0'(r)}{r} \leq 1$. The reason for this restriction will become apparent in the sequel, see Remark 3.1.

2.1. Eulerian dynamics and the spectral dynamics. The damped EMA system belongs to the broad class of pressureless Eulerian dynamics

$$\begin{aligned} \partial_t \rho + \nabla \cdot (\rho \mathbf{u}) &= 0, \\ \partial_t (\rho \mathbf{u}) + \nabla \cdot (\rho \mathbf{u} \otimes \mathbf{u}) &= \rho \mathbf{F}, \end{aligned}$$

where $\mathbf{F} := -\kappa \nabla \phi - \beta \mathbf{u}$ denotes the forcing term and ϕ is the potential that satisfies the Monge-Ampère equation (1.1c). In the non-vacuous region, the momentum equation (1.1b) simplifies to

$$(2.4) \quad \partial_t \mathbf{u} + (\mathbf{u} \cdot \nabla) \mathbf{u} = \mathbf{F}.$$

Under the assumption of radial symmetry, the force \mathbf{F} is expressed as

$$\mathbf{F}(\mathbf{x}, t) = \kappa \frac{\mathbf{x}}{r} \partial_r \phi(r, t) - \beta \frac{\mathbf{x}}{r} u(r, t),$$

which ensures the persistence of radial symmetry over time. Furthermore, let U be defined as

$$(2.5) \quad U(\mathbf{x}, t) := \int_0^{|\mathbf{x}|} u(s, t) \, ds.$$

We observe that $\mathbf{u}(\mathbf{x}, t) = \nabla U(\mathbf{x}, t)$, implying the no-swirl (irrotational) solutions persist in time as well.

2.1.1. *1D motivation and Riccati structure.* If $\mathbf{F} \equiv 0$, (2.4) reduces to the classical *inviscid Burgers equation*. It is well known that the solution leads to finite-time shock formation for any generic smooth initial data. Indeed, in one dimension, taking the spatial derivative of the equation yields

$$(\partial_t + u\partial_x)(\partial_x u) = -(\partial_x u)^2.$$

Let $X(t) = X(t; x)$ denote the characteristics originating from $x \in \mathbb{R}$, defined by

$$\frac{d}{dt}X(t) = u(X(t), t), \quad X(0) = x.$$

Let $'$ be the derivative along the characteristic path

$$f'(t) := \frac{d}{dt}f(X(t), t) = \partial_t f(X(t), t) + u(X(t), t) \partial_x f(X(t), t).$$

we obtain $(\partial_x u(X(t), t))' = -(\partial_x u(X(t), t))^2$. This is a Riccati type equation that encodes the solution structure: blowup occurs in a finite time if $\partial_x u_0(x) < 0$. The Riccati structure based analysis has been extended to various models, for example, see [26, 3, 23, 33, 4, 13, 9, 12].

2.1.2. *Spectral dynamics in Multidimensions.* To extend the above approach to multidimensions, we take the spatial gradient of (2.4) and obtain

$$(2.6) \quad (\partial_t + \mathbf{u} \cdot \nabla) \nabla \mathbf{u} + (\nabla \mathbf{u})^2 = \nabla \mathbf{F}.$$

The uniform boundedness of the n -by- n velocity gradient matrix $\|\nabla \mathbf{u}(\cdot, t)\|_{L^\infty}$ is of particular importance, since in many cases, this quantity plays a significant role in establishing global regularity.

A natural candidate for capturing the 1D Riccati structure in higher dimensions is the set of eigenvalues of the velocity gradient $\nabla \mathbf{u}$, denoted by $\{\lambda_i\}_{i=1}^n$. In the unforced case $\mathbf{F} \equiv 0$, the dynamics of λ_i , known as the *spectral dynamics*, exhibits the same Riccati structure as $\partial_x u$. Indeed, we observe

$$(\partial_t + \mathbf{u} \cdot \nabla) \lambda_i = -\lambda_i^2, \quad i = 1, \dots, n,$$

which can be explicitly solved along the characteristics path. This approach was thoroughly studied in [24]. While the dynamics of $\{\lambda_i\}_{i=1}^n$ enjoys the explicit Riccati structure, in the presence of nontrivial forcing terms, the spectral dynamics of (2.6) becomes

$$(2.7) \quad (\partial_t + \mathbf{u} \cdot \nabla) \lambda_i = -\lambda_i^2 + \langle \mathbf{l}_i, (\nabla \mathbf{F}) \mathbf{r}_i \rangle \quad i = 1, \dots, n,$$

where $(\mathbf{l}_i, \mathbf{r}_i)$ are the corresponding left and right eigenvectors of λ_i . We face an immediate problem of controlling the term $\langle \mathbf{l}_i, (\nabla \mathbf{F}) \mathbf{r}_i \rangle$. As the forcing gradient $\nabla \mathbf{F}$ may not share the same eigen-system as $\nabla \mathbf{u}$.

However, in the radial symmetry setting, the two matrices turn out to share the same eigen-system (see Lemma 3.1). This allows for the study of the spectral dynamics associated with (2.6). More precisely, we will analyze the dynamics of the following quantities

$$\left(u'_0(|\mathbf{x}|), \frac{u_0(|\mathbf{x}|)}{|\mathbf{x}|}, \phi''_0(|\mathbf{x}|), \frac{\phi'_0(|\mathbf{x}|)}{|\mathbf{x}|} \right).$$

In particular, as established in Lemma 3.2, the uniform boundedness of these quantities are key to global regularity.

2.1.3. *The divergence approach.* An alternative multidimensional analogue to $\partial_x u$ is *the divergence*

$$d := \nabla \cdot \mathbf{u} = \text{trace}(\nabla \mathbf{u}) = \sum_i^n \lambda_i.$$

Taking the trace of the (2.6) yields its dynamics:

$$(2.8) \quad (\partial_t + \mathbf{u} \cdot \nabla) d = -\text{trace}((\nabla \mathbf{u})^{\otimes 2}) + \nabla \cdot \mathbf{F}.$$

While d is real-valued and couples more easily to forcing terms, as $\nabla \cdot \mathbf{F}$ is typically simpler to control than $l_i^T(\nabla \mathbf{F})r_i$, the explicit Riccati structure is lost because $\text{trace}((\nabla \mathbf{u})^{\otimes 2}) \neq d^2$, for $n \geq 2$. The discrepancy is governed by the *spectral gap* of the matrix $\nabla \mathbf{u}$, defined as

$$(2.9) \quad \eta = \frac{1}{2} \sum_{i=1}^n \sum_{j=1}^n (\lambda_i - \lambda_j)^2.$$

This gives

$$(2.10) \quad d^2 - \text{trace}((\nabla \mathbf{u})^{\otimes 2}) = \frac{n-1}{n} d^2 - \frac{1}{n} \eta.$$

To extend 1D regularity result and utilize the Riccati structure via the divergence d , one must additionally control the spectral gap, which is often a delicate and difficult task. For instance, one approach involves decomposing the velocity gradient $\nabla \mathbf{u}$ into its symmetric and anti-symmetric part and controlling the spectral gaps of these two matrices individually, as demonstrated in [20]. Further discussions on the dynamics of the divergence d can be found [33, Remark 2.3, Remark 2.6].

In the radially symmetric setting, the divergence simplifies to

$$(2.11) \quad d = \nabla \cdot \mathbf{u} = u_r + (n-1) \frac{u}{r}.$$

Then we find that the discrepancy in (2.10) becomes

$$(2.12) \quad d^2 - \text{trace}((\nabla \mathbf{u})^{\otimes 2}) = 2(n-1)u_r \frac{u}{r} + (n-1)(n-2) \frac{u^2}{r^2}.$$

Because d is a weighted sum of u_r and u/r , this term involves quadratic expressions of u_r and $\frac{u}{r}$ which cannot be determined solely by the *local information* of d . However, a key observation is that under the radial symmetry, both the divergence of the spectral gap can be fully determined by u_r and $\frac{u}{r}$. In fact, the spectral gap simplifies greatly to $\eta = \frac{1}{n-1}(u_r - \frac{u}{r})^2$. Furthermore, unwrapping the divergence evolution equation (2.8) gives

$$\left(u_r + (n-1) \frac{u}{r} \right)' = -u_r^2 - (n-1) \frac{u^2}{r^2} - \kappa \phi'' - \kappa(n-1) \frac{\phi'}{r} - \beta u_r - (n-1) \beta \frac{u}{r},$$

where $'$ is the derivative along the characteristic path. This structure suggests the importance of the pairs $(u_r, \frac{u}{r})$ and $(\phi'', \frac{\phi'}{r})$. We will see shortly in Lemma 3.1 that they are precisely the eigenvalues of the velocity gradient $\nabla \mathbf{u}$ and the potential Hessian $D^2 \phi$, respectively. As it turns out, controlling these four quantities is key to global regularity. This leads to the first result of this paper.

2.2. Local well-posedness. We state the following local well-posedness and regularity criterion result for the damped EMA system.

Theorem 2.1 (Local well-posedness). *Let $s > \frac{n}{2}$. Consider the damped EMA system (1.1) with smooth radial initial data of the form*

$$(2.13) \quad \rho_0(\mathbf{x}) = \rho_0(r), \quad \mathbf{u}_0(\mathbf{x}) = \frac{\mathbf{x}}{r} u_0(r), \quad \phi_0(\mathbf{x}) = \phi_0(r), \quad r = |\mathbf{x}|.$$

Assume

$$\boldsymbol{\Omega}_0(|\mathbf{x}|) := \left[u'_0(|\mathbf{x}|), \frac{u_0(|\mathbf{x}|)}{|\mathbf{x}|}, \phi''_0(|\mathbf{x}|), \frac{\phi'_0(|\mathbf{x}|)}{|\mathbf{x}|} \right]^\top \in (H^s(\mathbb{R}^n))^4, \quad s > \frac{n}{2}.$$

Then there exists a time $T > 0$ such that the solution $\boldsymbol{\Omega}(\mathbf{x}, t)$ satisfies

$$(2.14) \quad \boldsymbol{\Omega}(|\mathbf{x}|, t) \in C([0, T], H^s(\mathbb{R}^n))^4.$$

Moreover, the life span T can be extended as long as

$$(2.15) \quad \int_0^T \|\boldsymbol{\Omega}(\cdot, t)\|_{L^\infty} dt < +\infty.$$

The statement of the theorem is a direct consequence of an a priori estimate. For the sake of completeness, we provide a proof of this result in Appendix A.

2.3. Global regularity versus finite time blowup. The next main result of this work concerns the phenomenon of critical thresholds. As implied by the regularity criterion (2.15), the global regularity depends on the boundedness of $\boldsymbol{\Omega}(\mathbf{x}, t)$. In this paper, we demonstrate that the damped EMA system (1.1) exhibits a *sharp* and *explicit* critical threshold. Specifically, subcritical initial data ensure $\boldsymbol{\Omega}$ remain bounded for all time, leading to global well-posedness via Theorem 2.1. On the contrary, supercritical initial data results in finite time singularity formation, where the velocity gradient and density lose uniform boundedness.

We provide a more precise and explicit characterization of these threshold conditions via two equivalent constructions. The first, in Section 4, utilizes a direct phase plane analysis of the explicit solutions to the spectral dynamics. In particular, we characterize the threshold conditions both in the *vacuous* and *non-vacuous* settings, see Theorem 4.2 and 4.1. The second, in Section 5, employs a comparison principle based on a Lyapunov function approach.

Theorem 2.2 (Critical thresholds). *Consider the damped EMA system (1.1) with radial symmetry (2.1). The following results hold:*

- *Global well-posedness: there exists a subcritical region $\widehat{\Sigma}_b \subset \mathbb{R} \times \mathbb{R}$, such that if the initial data satisfy*

$$(u'_0(r), \phi''_0(r)) \in \widehat{\Sigma}_b, \quad \forall r > 0,$$

then the damped EMA system (1.1) has a unique global smooth solution, in the sense that (2.14) holds for all time T .

- *Finite time singularity formation: there exists a supercritical region $\widehat{\Sigma}_\sharp = \widehat{\Sigma}_b^c$, such that if the initial data satisfy*

$$\exists r_* > 0 \text{ such that } (u'_0(r_*), \phi''_0(r_*)) \in \widehat{\Sigma}_\sharp,$$

then smooth solution to the damped EMA system (1.1) only exists for $t \in [0, T_]$ and moreover, the solution generates a singular shock at the blowup time T_* and location*

$r_c = r(T_c; r_0)$, namely

$$(2.16) \quad \lim_{t \rightarrow T_*^-} \partial_r u(r_*, t) = -\infty, \quad \lim_{t \rightarrow T_*^-} \rho(r_*, t) = \infty \text{ (or 0).}$$

2.4. Large-time behavior. The large-time dynamics of pressureless Eulerian systems have been recently discussed in [29, 8]. In particular, [8] provides a rigorous and comprehensive analysis of systems coupled with nonlocal velocity alignment and various interaction forces. In the presence of velocity damping, it is natural to anticipate the asymptotic convergence of global classical solutions toward an equilibrium state. In this work, we establish the large-time behavior for classical solutions to the damped EMA system (1.1), with optimal exponential rates of convergence.

Here, we use the notation $A \lesssim B$ to mean $A \leq CB$ for some positive constant C which depends on up to parameters β, κ , dimension n , the initial data and in the case of critically damped regime, some small $\varepsilon > 0$.

Theorem 2.3 (Large Time Behavior). *Let (ρ, \mathbf{u}, ϕ) be a global classical solution of (1.1). Then the following exponential decay holds for all $t \geq 0$:*

$$(2.17) \quad \|\nabla \mathbf{u}(\cdot, t), \mathbf{u}(\cdot, t), \rho(\cdot, t) - 1, \partial_r^2 \phi(\cdot, t), \partial_r \phi(\cdot, t)\|_{L^\infty(\mathbb{R}^n)} \lesssim e^{-\gamma t}.$$

The precise dependence of the decay rate γ on the parameters (β, κ) , the initial data and $\varepsilon > 0$ is provided in Theorem 4.3.

3. THE DAMPED EULER–MONGE–AMPÈRE SYSTEM WITH RADIAL SYMMETRY.

In this section, we discuss the implications of radial symmetry and derive the spectral dynamics for the damped EMA system (1.1). We first establish that, under radial symmetry, the velocity gradient $\nabla \mathbf{u}$ and the forcing gradient $\nabla \mathbf{F}$ share the same eigen-system. More generally, we show that the Hessians of all radially symmetric scalar fields share the same eigensystem.

Lemma 3.1. *Let $f : \mathbb{R}^n \rightarrow \mathbb{R}$ be a radial scalar function $f(\mathbf{x}) = f(r)$ with $r = |\mathbf{x}|$ and $f \in C^2((0, \infty))$. Then for any $\mathbf{x} \neq \mathbf{0}$, we have*

$$D^2 f(x) = \frac{f'(r)}{r} I + \left(f''(r) - \frac{f'(r)}{r} \right) \frac{xx^\top}{r^2}.$$

Moreover, $D^2 f(x)$ has eigenvalues

- $\lambda_1(D^2 f) = f''(r)$ associated with the eigenvector $\mathbf{v}_1 = \mathbf{x}$;
- $\lambda_i(D^2 f) = \frac{f'(r)}{r}$, $i = 2, \dots, n$, associated with $\{\mathbf{v}_2, \dots, \mathbf{v}_n\}$ which span $\{\mathbf{x}^\perp\}$.

Proof. Denoting $\partial_i = \frac{\partial}{\partial x_i}$, observe under the radial symmetry

$$\partial_i f(\mathbf{x}) = f'(r) \partial_i r = f'(r) \frac{x_i}{r}.$$

Differentiate again to obtain

$$\begin{aligned} \partial_{ij}^2 f(\mathbf{x}) &= f''(r) \frac{x_i x_j}{r^2} + f'(r) \frac{\delta_{ij}}{r} - \frac{x_i x_j}{r^3} \\ &= \frac{f'(r)}{r} \delta_{ij} + \left(f''(r) - \frac{f'(r)}{r} \right) \frac{x_i x_j}{r^2}. \end{aligned}$$

Write in matrix form to obtain

$$D^2 f(\mathbf{x}) = \frac{f'(r)}{r} I + \left(f''(r) - \frac{f'(r)}{r} \right) \frac{\mathbf{x}\mathbf{x}^\top}{r^2}.$$

We verify the eigen-system as stated in the lemma

$$\begin{aligned} (\lambda_1 I - D^2 f(\mathbf{x}))\mathbf{x} &= \left[\left(f''(r) - \frac{f'(r)}{r} \right) I - \left(f''(r) - \frac{f'(r)}{r} \right) \frac{\mathbf{x}\mathbf{x}^\top}{r^2} \right] \mathbf{x} \\ &= \left(f''(r) - \frac{f'(r)}{r} \right) \mathbf{x} - \left(f''(r) - \frac{f'(r)}{r} \right) \frac{\mathbf{x}\mathbf{x}^\top \mathbf{x}}{r^2} = 0, \\ (\lambda_2 I - D^2 f(\mathbf{x}))\mathbf{v}_i &= \left(f''(r) - \frac{f'(r)}{r} \right) \frac{\mathbf{x}\mathbf{x}^\top \mathbf{v}_i}{r^2} = 0, \quad \forall i \in \{2, \dots, n\}. \end{aligned}$$

The last line follows from $\mathbf{v}_i \in \mathbf{x}^\perp$, for all $i \in \{2, \dots, n\}$. This completes the proof. \square

Consequently, the velocity gradient and the forcing gradient

$$\nabla \mathbf{u}(\mathbf{x}, t) = D^2 U(r, t), \quad \nabla \mathbf{F}(\mathbf{x}, t) = -\kappa D^2 \phi(r) - \beta D^2 U(r, t),$$

share the same eigenvectors. Here, U is defined in (2.5). This fact allows us to utilize the explicit Riccati structure in the spectral dynamics (2.7). Hence, we propose to use the pair

$$(3.1) \quad (p(r, t), q(r, t)) := \left(\partial_r u(r, t), \frac{u(r, t)}{r} \right)$$

as the multidimensional analogue of $\partial_x u$ in 1D. Similarly, we use

$$(3.2) \quad (\mu(r, t), \nu(r, t)) := \left(\partial_r^2 \phi(r, t), \frac{\partial_r \phi(r, t)}{r} \right),$$

to denote the eigenvalues of the potential gradient $D^2 \phi(r, t)$.

Let $' := \partial_t + u(r, t) \partial_r$ denote differentiation along the characteristics paths, then the spectral dynamics (2.7) becomes

$$(3.3) \quad \begin{cases} p' = -p^2 - \kappa\mu - \beta p, \\ q' = -q^2 - \kappa\nu - \beta q. \end{cases}$$

A remarkable fact of studying the pair (p, q) is that the boundedness of the radial derivative $p = \partial_r u(r, t)$ is sufficient to guarantee the boundedness of $\nabla \mathbf{u}$, as demonstrated in the next lemma.

Lemma 3.2. *Consider the radial velocity field (2.1), (2.2), where $\mathbf{u}(\mathbf{x}, t) = \frac{\mathbf{x}}{r} u(r, t)$ and $u(0, t) = 0$. Then*

$$(3.4) \quad \|\nabla \mathbf{u}(\cdot, t)\|_{L^\infty} \leq \|\partial_r u(r, t)\|_{L^\infty}.$$

Proof. To verify (3.4) recall that $\nabla \mathbf{u}(\mathbf{x}, t)$ is given by the radial Hessian

$$\nabla \mathbf{u}(\mathbf{x}, t) = D^2 U(r) = q(r, t) I + (p(r, t) - q(r, t)) \frac{\mathbf{x}\mathbf{x}^\top}{r^2},$$

where $(p(r, t), q(r, t)) = (\partial_r u(r, t), \frac{u(r, t)}{r})$ is as defined in (3.3). Observe $\nabla \mathbf{u}$ thus defines a bilinear form. Let \mathbf{w} be an arbitrary unit vector, then we have

$$\langle \nabla \mathbf{u}(\mathbf{x}, t) \mathbf{w}, \mathbf{w} \rangle = q(r, t) \|\mathbf{w}\|^2 + (p(r, t) - q(r, t)) \langle \frac{\mathbf{x}\mathbf{x}^\top}{r^2} \mathbf{w}, \mathbf{w} \rangle$$

$$= q(r, t) + (p(r, t) - q(r, t)) \frac{\|\mathbf{x}^T \mathbf{w}\|^2}{r^2}.$$

Let $\theta = \frac{\|\mathbf{x}^T \mathbf{w}\|^2}{r^2}$, and observe $\theta \in [0, 1]$. Then

$$\langle \nabla \mathbf{u}(\mathbf{x}, t) \mathbf{w}, \mathbf{w} \rangle = (1 - \theta)q + \theta p \leq \max\{p, q\}.$$

Moreover, by (2.2), $u(0, t) = 0$ and hence

$$|q(r, t)| = \frac{1}{r} \left| \int_0^r \partial_s u(s, t) \, ds \right| \leq \|p(\cdot, t)\|_{L^\infty},$$

and the statement follows from the last two inequalities. \square

In a similar fashion, we establish a lemma that provides a uniform bound on ν . Combining this result with the spectral representation of the Monge–Ampère equation (1.1c) allows us to bound $\|\rho\|_{L^\infty}$ by the radial eigenvalue μ of the Hessian $D^2\phi$.

Lemma 3.3. *Let μ and ν be defined as in (3.2), and assume the boundary regularity 2.2, then we have*

$$(3.5) \quad \|\nu(\cdot, t)\|_{L^\infty} \leq \|\mu(\cdot, t)\|_{L^\infty}.$$

Proof. We observe

$$|\nu(r, t)| = \frac{1}{r} |\partial_r \phi(r, t)| = \frac{1}{r} \left| \int_0^r \partial_r^2 \phi(s, t) \, ds + \partial_r \phi(0, t) \right|.$$

Since $\partial_r \phi(0, t) = 0$, equation (3.5) holds. \square

3.1. Spectral dynamics for the radial damped Euler–Monge–Ampère system. In this section, we derive the spectral representation of the Monge–Ampère equation (1.1c) and the continuity equation (1.1a). These relations are essential for characterizing the dynamics of the eigenvalues (μ, ν) , which, as stated in Theorem 2.1, govern the global regularity of the system alongside the velocity gradient components (p, q) .

Lemma 3.4 (Spectral form of the Monge–Ampère equation). *Let (ρ, ϕ) satisfy the initial condition (2.1), (2.2) and the Monge–Ampère equation $\det(\mathbb{I} - D^2\phi) = \rho$. Let (μ, ν) be given as in (3.2). Then the following relations hold:*

- The density admits the pointwise spectral representation:

$$(3.6) \quad \rho = (1 - \mu)(1 - \nu)^{n-1}.$$

- The global mass distribution is characterized by the identity:

$$(3.7) \quad \partial_r(r^n(1 - \nu)^n) = nr^{n-1}\rho.$$

Proof. The first claim is straightforward to verify:

$$\rho = \det(\mathbb{I} - D^2\phi) = \prod_{i=1}^n (1 - \lambda_i(D^2\phi)) = (1 - \mu)(1 - \nu)^{n-1}.$$

Next, from the definition (3.2), we observe the following the differential relation between μ and ν :

$$\mu = \partial_r(r\nu) = r\partial_r\nu + \nu.$$

This implies $1 - \mu = 1 - \nu - r\partial_r\nu$. Substituting this equation into (3.6), we obtain

$$(1 - \mu)(1 - \nu)^{n-1} = (1 - \nu)^n - r\partial_r\nu(1 - \nu)^{n-1} = \frac{1}{nr^{n-1}}\partial_r(r^n(1 - \nu)^n).$$

This completes the proof. \square

Remark 3.1. Recall that we require the potential ϕ to satisfy the initial condition $\phi_0''(r) \leq 1$. This is a direct consequence of the spectral Monge–Ampère equation (3.6). In the one-dimensional case, (1.1c) reduces to $-\partial_{xx}\phi = \rho - 1$; thus, the physical requirement of non-negative initial density, $\rho_0 \geq 0$, is equivalent to $\phi_0''(r) \leq 1$. In higher dimensions, the relationship between the non-negativity of ρ_0 and the bounds on $\phi_0''(r)$ becomes dimension-dependent. Specifically, if $\phi_0''(r) = \mu_0 > 1$, then (2.2) implies that $\phi_0'(r)/r = \nu_0 > 1$ as well; consequently, the sign of ρ_0 depends on the parity of the dimension n . Furthermore, as discussed in Remark 4.3, the condition $\phi_0''(r) > 1$ yields universal blow-up phenomenon. To ensure physical consistency, we enforce the condition $\phi_0''(r) \leq 1$.

Lemma 3.5 (Spectral form of the continuity equation). *Let $\rho(\mathbf{x}, t)$ and $\mathbf{u}(\mathbf{x}, t)$ be as given in (2.1) and (2.2). Under radial symmetry, the evolution of the density (1.1a) becomes*

$$(3.8) \quad \partial_t\rho + \partial_r(\rho u) = -\frac{(n-1)\rho u}{r}.$$

Proof. First observe by radial symmetry, we have

$$\begin{aligned} \nabla \cdot (\rho \mathbf{u}) &= \sum_{i=1}^n \partial_i \left(\rho u \frac{x_i}{r} \right) \\ &= \sum_{i=1}^n \partial_r(\rho u) \frac{x_i^2}{r} + \sum_{i=1}^n \rho u \left(\frac{1}{r} - \frac{x_i^2}{r^3} \right) \\ &= \partial_r(\rho u) + \frac{(n-1)\rho u}{r}. \end{aligned}$$

Hence the continuity equation (1.1a) becomes

$$\partial_t\rho + \nabla \cdot (\rho \mathbf{u}) = \partial_t\rho + \partial_r(\rho u) + \frac{(n-1)\rho u}{r} = 0.$$

This completes the proof. \square

Let us discuss several consequences of the above two lemmas, in particular, the dynamics of ν .

Lemma 3.6. *Let $\rho = \rho(r, t)$ and $u = u(r, t)$ be smooth radial solutions of the continuity equation (3.8) and define*

$$e(r, t) := \int_0^r s^{n-1} \rho(s, t) ds.$$

Let $' = \partial_t + u\partial_r$ be material derivative along the characteristic path $\dot{r} = u(r, t)$. Then

$$e' = \partial_t e + u\partial_r e = 0, \quad \text{and} \quad (r(1 - \nu))' = 0,$$

where μ and ν are defined as in (3.2). Consequently

$$\nu' = q(1 - \nu),$$

where q is defined as in (3.1).

Proof. Multiplying the continuity equation (3.8) by r^{n-1} gives

$$r^{n-1} \partial_t \rho + r^{n-1} \partial_r (\rho u) = -(n-1) r^{n-2} \rho u.$$

this is equivalent to

$$(3.9) \quad \partial_t (r^{n-1} \rho) + \partial_r (r^{n-1} \rho u) = 0.$$

By definition of $e(r, t)$ we obtain

$$\partial_t e(r, t) = \int_0^r s^{n-1} \partial_t \rho(s, t) ds, \quad \partial_r e(r, t) = r^{n-1} \rho(r, t).$$

Integrating (3.9) over $[0, r]$ to obtain

$$\partial_t e(r, t) + r^{n-1} \rho(r, t) u(r, t) = 0.$$

Let $r = r(t; r_0)$ be the characteristic path initiated at r_0 , satisfying $r' = u(r, t)$, $r(0; r_0) = r_0$. This gives

$$\partial_t e + u \partial_r e = e'(r, t) = 0.$$

Next, we derive the dynamics of ν . Observe from (3.7), we get $r^n (1-\nu)^n = ne$. The conclusion that $e' = 0$ then implies that $(r(1-\nu))' = 0$. Consequently, we have the dynamics of ν

$$(3.10) \quad \nu' = \frac{r'}{r} (1-\nu) = \frac{u}{r} (1-\nu) = q(1-\nu).$$

□

Combining with the previously derived evolution equations for (p, q) (3.3), we observe that the dynamics of (q, ν) forms a closed ODE system along the characteristic paths

$$(3.11) \quad \begin{cases} q' = -q^2 - \kappa \nu - \beta q, \\ \nu' = q(1-\nu). \end{cases}$$

Crucially, the dynamics of (p, μ) satisfies a system of the identical form. To see this, recall the spectral representation of the mass continuity equation (3.8)

$$(3.12) \quad \partial_t \rho + u \partial_r \rho = -\rho \partial_r u - \frac{(n-1)\rho u}{r}.$$

Along the characteristic path the dynamics of ρ becomes

$$(3.13) \quad \rho' = -\rho(p + (n-1)q).$$

Furthermore, the spectral form of the Monge-Ampère equation (3.6) implies

$$\mu = 1 - \frac{\rho}{(1-\nu)^{n-1}}.$$

This together with (3.10), yields

$$\begin{aligned} \mu' &= -\frac{\rho'(1-\nu)^{n-1} + (n-1)\rho(1-\nu)^{n-2}\nu'}{(1-\nu)^{2n-2}} = -\frac{-\rho(p + (n-1)q) + (n-1)\rho q}{(1-\nu)^{n-1}} \\ &= \frac{\rho p}{(1-\nu)^{n-1}} = p(1-\mu). \end{aligned}$$

Therefore, the dynamics of (p, μ) also forms a closed ODE system along the characteristic paths

$$(3.14) \quad \begin{cases} p' = -p^2 - \kappa \mu - \beta p, \\ \mu' = p(1-\mu). \end{cases}$$

As established by Lemma 3.2 and 3.5, since the tangential pair (q, ν) and the radial pair (p, μ) are governed by the identical ODE systems, the global regularity of the damped EMA system is entirely determined by the dynamics of (p, μ) . Consequently, the threshold conditions and asymptotic behavior results derived for the radial components apply directly to the tangential components.

4. PROOF OF THE MAIN RESULTS.

In this section, we aim to construct the sharp critical threshold regions in the (p, μ) , which in turns characterizes the necessary and sufficient conditions ensuring the uniform boundedness of $\nabla \mathbf{u}$ and ρ , both in the vacuous and non-vacuous scenarios. In the second scenario, we apply a transform that reformulates (3.14) into a system of linear ODEs, which enables us to perform explicit phase analysis. This approach also illuminates the explicit decay rate to equilibrium, hence we conclude the large-time asymptotic behavior. In the next section, we demonstrate a Lyapunov function based approach, utilizing the same transform.

Remark 4.1. As noted in the derivation of the Burgers–type equation (2.4), the reduction is based on the assumption of positive initial mass. Hence we emphasize that the critical threshold investigated in the vacuous setting is should be regarded as formal.

4.1. A vacuous critical threshold. Recall that condition (2.3) requires $\phi_0''(r) \leq 1$. We first consider the case $\phi_0''(r) = 1$, which corresponds to an initial vacuum $\rho_0 = 0$, as indicated (3.6). In the absence of damping, a density lower bound $\rho_0 \geq 2^{-n}$, where n is the dimension, is a necessary condition for global regularity. As a consequence, the undamped EMA system necessarily develops singular shocks in finite-time from a vacuous state, see [31]. We include a brief discussion of the density lower bound in remark 4.2. In what follows, we show that the introduction of damping can prevent the formation of these shocks.

From the evolution of μ in (3.14), we have:

$$\mu(t) = 1 - (1 - \mu_0)e^{-\int_0^t p(s) \, ds}.$$

Setting $\mu_0 = \phi_0''(r) = 1$ implies that $\mu(t) = 1$ for all $t > 0$. Then in (3.14), the dynamics of p simplifies to the autonomous Riccati ODE:

$$(4.1) \quad p' = -p^2 - \beta p - \kappa.$$

Depending on the damping coefficient β , we have three scenarios:

(I) *Strong damping* ($\beta > 2\sqrt{\kappa}$). In this regime, $p(t)$ has two fixed points $p_- < p_+ < 0$, corresponding to the two real roots of the polynomial $f(p) = p^2 + \beta p + \kappa = 0$:

$$p_- = \frac{-\beta - \sqrt{\beta^2 - 4\kappa}}{2}, \quad \text{and} \quad p_+ = \frac{-\beta + \sqrt{\beta^2 - 4\kappa}}{2}.$$

Observe $f(p)$ is a downward-opening parabola; thus, for any initial data $p_0 \in [p_-, \infty)$, the solution $p(t)$ is bounded and asymptotically approaches the stable equilibrium p_+ . Conversely, for any $p_0 < p_-$, the quadratic growth of the $-p^2$ term dominates, and $p(t)$ diverges to $-\infty$ in finite time $t = T_c$. To see that T_c is finite, we integrate (4.1) and obtain

$$T_c = \int_0^{T_c} dt = \int_{p_0}^{-\infty} \frac{dp}{-p^2 - \beta p - \kappa}$$

$$= \int_{p_0}^{-\infty} -\frac{dp}{(p-p_-)(p-p_+)} = \frac{1}{p_+ - p_-} \ln \left| \frac{p_0 - p_+}{p_0 - p_-} \right|.$$

Since $p_0 < p_- < p_+$, T_c is positive and finite.

(II) *Critical damping* ($\beta = 2\sqrt{\kappa}$). In this case, the polynomial $f(p) = -p^2 - \beta p - \kappa$ has one real root $p_* = -\beta/2 = -\sqrt{\kappa}$. Following a similar analysis, we conclude that if $p_0 \in [p_*, \infty)$, then $p(t)$ remains bounded and approaches the equilibrium p_* . For $p_0 < p_*$, $p(t)$ approaches $-\infty$ in finite time. To see this, we observe

$$T_c = \int_{p_0}^{-\infty} \frac{dp}{-p^2 - \beta p - \kappa} = \int_{p_0}^{-\infty} \frac{dp}{-p^2 - 2\sqrt{\kappa}p - \kappa} = \int_{p_0}^{-\infty} \frac{dp}{-(p + \sqrt{\kappa})^2} = -\frac{1}{p_0 + \sqrt{\kappa}}.$$

Since $p_0 < p_* = -\sqrt{\kappa}$, we see that T_c is positive and finite.

(III) *Weak damping* ($\beta < 2\sqrt{\kappa}$). In this case, the polynomial $f(p) = -p^2 - \beta p - \kappa$ doesn't have a real root. All initial data p_0 lead to blow-up at a finite time T_c determined by the following integral

$$\begin{aligned} T_c &= \int_{p_0}^{-\infty} \frac{dp}{-p^2 - \beta p - \kappa} = \int_{p_0}^{-\infty} -\frac{dp}{(p + \beta/2)^2 + (\sqrt{\kappa - \beta^2/4})^2} \\ &= \frac{1}{\sqrt{\kappa - \beta^2/4}} \left[\arctan \left(\frac{p_0 + \beta/2}{\sqrt{\kappa - \beta^2/4}} \right) + \frac{\pi}{2} \right]. \end{aligned}$$

Indeed, the above integral is finite for any initial data p_0 , implying that in the weakly damped regime, every smooth initial data experiences finite time singularity formation.

In conclusion, we have the following characterization of the sharp and explicit critical threshold in vacuum.

Theorem 4.1. *Consider the damped EMA system (1.1) with radial symmetry (2.1), and initial data (1.2) satisfying (2.2). In addition, suppose the potential ϕ satisfies $\phi_0''(r) = 1$ for all $r > 0$, implying a vacuous state of density. If the initial condition satisfies*

- *Strong damping* ($\beta > 2\sqrt{\kappa}$)

$$u_0'(r) \geq \frac{-\beta - \sqrt{\beta^2 - 4\kappa}}{2}, \quad \forall r > 0.$$

- *Critical damping* ($\beta = 2\sqrt{\kappa}$)

$$u_0'(r) \geq -\sqrt{\kappa}, \quad \forall r > 0.$$

then $\nabla \mathbf{u}$ is uniformly bounded for all time. Conversely, $\nabla \mathbf{u}$ develops a (non-physical) singular shock at time T_c and location $r_c = r(T_c; r_0)$, namely

$$(4.2) \quad \lim_{t \rightarrow T_c^-} \partial_r u(r_c, t) = -\infty, \quad \lim_{t \rightarrow T_c^-} \rho(r_c, t) = 0.$$

In addition, any smooth initial data generate singular shock in finite time in the weakly damped regime.

The proof of theorem 4.2 contains the above as a special case.

4.2. A non-vacuous critical threshold. Here we deal with the second case where $\phi_0''(r) = \mu_0 < 1$. This allows us to take advantage of the following two new variables.

$$(4.3) \quad w := \frac{p}{1-\mu}, \quad s := \frac{1}{1-\mu}.$$

The new pair of variables leads to a reformed coupled system, whose dynamics can be derived from (3.14):

$$\begin{aligned} w' &= \frac{p'(1-\mu) + p\mu'}{(1-\mu)^2} = \frac{(-p^2 - \kappa\mu - \beta p)(1-\mu) + p^2(1-\mu)}{(1-\mu)^2} = \kappa(1-s) - \beta w, \\ s' &= \frac{\mu'}{(1-\mu)^2} = \frac{p}{1-\mu} = w. \end{aligned}$$

Hence, the dynamics of (w, s) is given by

$$(4.4) \quad \begin{cases} w' = -\beta w + \kappa(1-s), \\ s' = w. \end{cases}$$

Observe that the forcing terms in the right hand of (4.4) are Lipschitz in (w, s) , which ensures that the solution $(w(t), s(t))$ remains bounded for all finite time, see (4.6) and subsequent phase plane analysis. Furthermore, the solution $(w(t), s(t))$ decays in time. Since p can be recovered via $p = \frac{w}{s}$, the only possible finite-time blowup scenario in the (p, μ) plane is when $s(T_c) = 0$. To characterize the conditions under which this occurs, we partition the (w, s) phase plane into the following threshold regions:

- *Subcritical region* Σ_b : if $(w_0, s_0) \in \Sigma_b$, then $s(t) > 0$ for all time.
- *Supercritical region* Σ_\sharp : if $(w_0, s_0) \in \Sigma_\sharp$, then there exists a finite time $T_* > 0$ such that $s(T_*) = 0$.

The threshold regions in the (p, μ) plane can be recovered from those in the (w, s) plane. To this end, consider the Lyapunov function

$$(4.5) \quad \mathcal{L}(w, s) = w^2 + \kappa(1-s)^2.$$

Differentiating $\mathcal{L}(w, s)$ using the dynamics (4.4) gives

$$(4.6) \quad \frac{d}{dt} \mathcal{L}(w(t), s(t)) = 2ww' - 2\kappa(1-s)s' = -2\beta w^2,$$

implying that $(w(t), s(t))$ decays toward the equilibrium $(0, 1)$ in time. This Lyapunov function was introduced in [31] to investigate the critical threshold in the undamped case ($\beta = 0$). In that setting, $\frac{d}{dt} \mathcal{L}(w(t), s(t)) = 0$, and the trajectories of (4.4) trace ellipses in the phase plane. The critical threshold is identified by the level set passing through the origin $(0, 0)$, which corresponds to $\mathcal{L}(w(t), s(t)) = \mathcal{L}(w_0, s_0) = \kappa$. Consequently, the condition $s(t) > 0$ holds for all time provided the initial data satisfy $\mathcal{L}(w_0, s_0) < \kappa$, or equivalently, $|p_0| < \sqrt{\kappa(1 - 2\mu_0)}$.

Geometrically, the subcritical region in the undamped case is characterized as the interior region bounded by the ellipse centered at $(0, 1)$ that intersects the origin. We now present two equivalent constructions of the critical threshold: one utilizing explicit solutions to the system (4.4), and the other via a Lyapunov function based approach.

4.3. Explicit phase plane analysis. In our case, the introduction of the damping term renders integral curves to the system (4.4) non-closed. We can explicitly construct the thresholds in $(w(t), s(t))$ plane by solving (4.4). To this end, consider the following system of ODEs

$$\begin{bmatrix} w \\ s-1 \end{bmatrix}' = \begin{bmatrix} -\beta & -\kappa \\ 1 & 0 \end{bmatrix} \begin{bmatrix} w \\ s-1 \end{bmatrix},$$

subject to initial conditions

$$s(0) = s_0 = \frac{1}{1 - \mu_0}, \quad w(0) = w_0 = \frac{p_0}{1 - \mu_0}.$$

Let us denote

$$\lambda_1 := \frac{\beta - \sqrt{\beta^2 - 4\kappa}}{2}, \quad \lambda_2 := \frac{\beta + \sqrt{\beta^2 - 4\kappa}}{2}.$$

We observe $-\lambda_1$ and $-\lambda_2$ are the two eigenvalues of the coefficient matrix. If $\beta < 2\sqrt{\kappa}$, then λ_1 and λ_2 are complex-valued, with

$$\lambda_1 = \alpha - i\omega, \quad \lambda_2 = \alpha + i\omega, \quad \text{where } \alpha = \frac{\beta}{2}, \quad \text{and } \omega := \frac{1}{2}\sqrt{4\kappa - \beta^2}.$$

For analysis convenience, we also use the following second-order ODE, obtained by differentiating $s(t)$,

$$(4.7) \quad \begin{cases} s''(t) + \beta s'(t) + \kappa s(t) = \kappa, \\ s(0) = s_0, \quad s'(0) = w_0. \end{cases}$$

Throughout, we will use $s'(t)$ and $w(t)$ interchangeably, with the understanding that they denote the same function. There are three scenarios:

(I) *Strong damping* ($\beta > 2\sqrt{\kappa}$). The solution takes the following form

$$(4.8a) \quad s(t) = 1 + A_1 e^{-\lambda_1 t} + A_2 e^{-\lambda_2 t},$$

$$(4.8b) \quad w(t) = -A_1 \lambda_1 e^{-\lambda_1 t} - A_2 \lambda_2 e^{-\lambda_2 t}.$$

The coefficients A_1, A_2 are determined by the initial data:

$$A_1 = \frac{w_0 + \lambda_2(s_0 - 1)}{\lambda_2 - \lambda_1}, \quad A_2 = \frac{-w_0 - \lambda_1(s_0 - 1)}{\lambda_2 - \lambda_1}.$$

Recall by (4.4), $w(t) = s'(t)$. We first observe $s(t)$ can have at most one extremum. Let t^* be the time at which s attains the extremum. Setting $s'(t^*) = 0$, we find

$$(4.9) \quad e^{(\lambda_2 - \lambda_1)t^*} = -\frac{A_2 \lambda_2}{A_1 \lambda_1}, \quad \text{and} \quad t^* = \frac{1}{\lambda_2 - \lambda_1} \ln \left(-\frac{A_2 \lambda_2}{A_1 \lambda_1} \right).$$

Therefore, an extremum exists if and only if A_1 and A_2 have opposite signs. On the other hand, if there doesn't exist an extremum, then $s(t)$ decays monotonically in time to 1, and the positivity of $s(t)$ for all $t > 0$ holds if $s_0 > 0$, which is guaranteed by (2.3). Suppose the extremum exists, then a second derivative calculation yields

$$s''(t) = A_1 \lambda_1^2 e^{-\lambda_1 t} + A_2 \lambda_2^2 e^{-\lambda_2 t}.$$

At $t = t^*$, (4.9) gives

$$s''(t^*) = -(\lambda_2 - \lambda_1) A_1 \lambda_1 e^{-\lambda_1 t^*}.$$

We distinguish two cases based on the initial data:

- (1) If $A_1 > 0$ and $A_2 < 0$, then $s(t^*)$ is a local maximum. In this case $s(t^*)$ is bounded below by $\min\{s_0, 1\}$.
- (2) If $A_1 < 0$ and $A_2 > 0$, then $s(t^*)$ is a local minimum.

Therefore, a violation of $s(t) > 0$ can only occur if s possesses a local minimum at some $t^* > 0$. Observe (4.7) asserts $s''(t^*) + \kappa s(t^*) = \kappa$, implying

$$s(t^*) = \frac{\kappa - s''(t^*)}{\kappa}.$$

Consequently, the positivity of $s(t^*)$ is equivalent to the condition $s''(t^*) < \kappa$. On substituting the expression of t^* , we have

$$-A_1\lambda_1(\lambda_2 - \lambda_1) \left(-\frac{A_2\lambda_2}{A_1\lambda_1} \right)^{-\frac{\lambda_1}{\lambda_2 - \lambda_1}} < \kappa.$$

Further simplification using $A_1 < 0, A_2 > 0$ gives

$$\left[\frac{(\lambda_2 - \lambda_1)(-A_1\lambda_1)}{\kappa} \right]^{\lambda_2} < \left[\frac{(\lambda_2 - \lambda_1)A_2\lambda_2}{\kappa} \right]^{\lambda_1}.$$

Substituting the expression of A_1 and A_2 into the inequality yields

$$\left[-\frac{\lambda_1 w_0 + \kappa(1 - s_0)}{\kappa} \right]^{\lambda_2} < \left[-\frac{\lambda_2 w_0 + \kappa(1 - s_0)}{\kappa} \right]^{\lambda_1}.$$

In addition, the conditions $A_1 < 0$ and $A_2 > 0$ require

$$w_0 + \lambda_2(s_0 - 1) < 0, \quad w_0 + \lambda_1(s_0 - 1) < 0.$$

In terms of (p_0, μ_0) , the critical threshold condition becomes

$$(4.10) \quad \left[-\frac{\lambda_1 p_0 + \kappa \mu_0}{\kappa(1 - \mu_0)} \right]^{\lambda_2} < \left[-\frac{\lambda_2 p_0 + \kappa \mu_0}{\kappa(1 - \mu_0)} \right]^{\lambda_1}.$$

given

$$(4.11) \quad \frac{p_0 + \lambda_2 \mu_0}{1 - \mu_0} < 0, \quad \text{and} \quad \frac{p_0 + \lambda_1 \mu_0}{1 - \mu_0} < 0.$$

To summarize, a violation of $s(t) > 0$ in the strong damping regime, corresponding to a blow-up scenario in the main system (1.1), occurs if and only if the initial condition (p_0, μ_0) satisfies (4.11) but fails to meet the inequality (4.10). In particular, (4.11) simplifies to $p_0 + \lambda_2 \mu_0 < 0$ and $p_0 + \lambda_1 \mu_0 < 0$, as $1 - \mu_0$ is assumed to be positive (see remark (4.3)).

(II) *Critical damping* ($\beta = 2\sqrt{\kappa}$). The solution to the system (4.4) takes the form

$$(4.12a) \quad s(t) = 1 + \left[(s_0 - 1) + (w_0 + \alpha(s_0 - 1))t \right] e^{-\alpha t},$$

$$(4.12b) \quad w(t) = \left[w_0 - \alpha(w_0 + \alpha(s_0 - 1))t \right] e^{-\alpha t}.$$

We observe that $s(t)$ admits at most one local extremum. If no such extremum exists, $s(t)$ decays monotonically in time to 1, implying that $s(t)$ is bounded below by $\min\{s_0, 1\}$. Suppose instead that a local extremum exists at $t^* > 0$. Setting (4.12b) to 0 yields

$$t^* = \frac{w_0}{\alpha(w_0 + \alpha(s_0 - 1))}$$

For $t^* > 0$, the signs of w_0 and $w_0 + \alpha(s_0 - 1)$ must coincide. Evaluating the second derivative at $t = t^*$ gives

$$s''(t^*) = -\alpha(w_0 + \alpha(s_0 - 1))e^{-\alpha t^*}.$$

We distinguish two cases based on the initial data:

- (1) If $w_0 + \alpha(s_0 - 1) > 0$ and $w_0 > 0$, then $s(t^*)$ is a local maximum. In this case $s(t^*)$ is bounded below by $\min\{s_0, 1\}$.
- (2) If $w_0 + \alpha(s_0 - 1) < 0$ and $w_0 < 0$, then $s(t^*)$ is a local minimum.

To ensure $s(t^*) > 0$ in the latter case, we require $s(t^*) > 0$. Substituting t^* into (4.12a), we obtain

$$s(t^*) = 1 + \frac{w_0 + \alpha(s_0 - 1)}{\alpha}e^{-\alpha t^*}.$$

The condition $s(t^*) > 0$ therefore is equivalent to

$$e^{-\alpha t^*} < -\frac{\alpha}{w_0 + \alpha(s_0 - 1)}.$$

Substituting the expression for t^* leads to the critical threshold inequality:

$$\frac{w_0}{w_0 + \alpha(s_0 - 1)} > \ln \left[-\frac{w_0 + \alpha(s_0 - 1)}{\alpha} \right],$$

provided that

$$w_0 < 0 \quad \text{and} \quad w_0 + \alpha(s_0 - 1) < 0.$$

In terms of p_0 and μ_0 , this condition is expressed as:

$$(4.13) \quad \frac{p_0}{p_0 + \alpha\mu_0} > \ln \left[-\frac{p_0 + \alpha\mu_0}{\alpha(1 - \mu_0)} \right],$$

provided $p_0 < 0$ and $p_0 + \alpha\mu_0 < 0$, where we used the assumption $1 - \mu_0 > 0$ again. To summarize, a violation of $s(t) > 0$ in the critical damping regime, corresponding to a blow-up scenario in the main system (1.1), occurs if and only if the initial condition (p_0, μ_0) satisfies $p_0 < 0$ and $p_0 + \alpha\mu_0 < 0$ but fails to meet the inequality (4.13).

(III) *Weak damping* ($\beta < 2\sqrt{\kappa}$). The solution takes the following form

$$(4.14a) \quad s(t) = 1 + e^{-\alpha t} \left[(s_0 - 1) \cos(\omega t) + \frac{w_0 + \alpha(s_0 - 1)}{\omega} \sin(\omega t) \right],$$

$$(4.14b) \quad w(t) = e^{-\alpha t} \left[w_0 \cos(\omega t) - \frac{\alpha w_0 + \kappa(s_0 - 1)}{\omega} \sin(\omega t) \right].$$

Since $s(t)$ decays to 1, it suffices to identify the conditions where the first local minimum of $s(t)$ is positive. To this end, we set $s'(t) = w(t) = 0$ and find

$$\tan(\omega t) = \frac{\omega w_0}{\alpha w_0 + \kappa(s_0 - 1)}.$$

At $t = t^*$, the second derivative calculation gives

$$s''(t^*) = \frac{-\kappa \cos(\omega t^*) e^{-\alpha t^*}}{\alpha w_0 + \kappa(s_0 - 1)} \left[(w_0 + \alpha(s_0 - 1))^2 + (\kappa - \alpha^2)(s_0 - 1)^2 \right].$$

Recall $\kappa - \alpha^2 = \frac{1}{4}(4\kappa - \beta^2) > 0$ holds in the weak damping regime. Consequently, to have that $s(t^*)$ is a local minimum requires

$$\operatorname{sgn}(\cos(\omega t^*)) = -\operatorname{sgn}(\alpha w_0 + \kappa(s_0 - 1)).$$

This gives us a sequence of minima. The first local minimum occurs at

$$(4.15) \quad \omega t^* = \beta_0 + \arctan \left[\frac{\omega w_0}{\alpha w_0 + \kappa(s_0 - 1)} \right],$$

where

$$\beta_0 = \begin{cases} 0, & \alpha w_0 + \kappa(s_0 - 1) < 0 \text{ and } w_0 < 0, \\ \pi, & \alpha w_0 + \kappa(s_0 - 1) > 0, \\ 2\pi, & \alpha w_0 + \kappa(s_0 - 1) < 0 \text{ and } w_0 > 0. \end{cases}$$

To find the critical threshold condition, we express $s(t)$ as

$$s(t) = 1 + Re^{-\alpha t} \cos(\omega t - \psi),$$

where

$$R = \sqrt{(s_0 - 1)^2 + \frac{(w_0 + \alpha(s_0 - 1))^2}{\omega^2}}, \quad \tan \psi = \frac{w_0 + \alpha(s_0 - 1)}{\omega(s_0 - 1)}.$$

At the first local minimum t^* , set $s'(t^*) = 0$ and solve for $\cos(\omega t - \psi)$ gives

$$(4.16) \quad s(t^*) = 1 - \frac{\omega}{\sqrt{\omega^2 + \alpha^2}} R e^{-\alpha t^*}.$$

This implies the positivity of $s(t^*)$ is equivalent to

$$\frac{\omega^2}{\omega^2 + \alpha^2} R^2 e^{-2\alpha t^*} < 1.$$

Since $\omega^2 + \alpha^2 = \kappa$, the above condition becomes

$$(w_0 + \alpha(s_0 - 1))^2 + \omega^2(s_0 - 1)^2 < \kappa e^{2\alpha t^*},$$

where t^* is given as in (4.15). We then obtain the critical threshold inequality in terms of (p_0, μ_0) ,

$$(4.17) \quad \left(\frac{p_0 + \alpha \mu_0}{1 - \mu_0} \right)^2 + \omega^2 \left(\frac{\mu_0}{1 - \mu_0} \right)^2 < \kappa e^{2\alpha t^*}.$$

To summarize, a violation of $s(t) > 0$ in the weak damping regime, corresponding to a blow-up scenario in the main system (1.1), occurs if and only if the initial condition (p_0, μ_0) fails to meet the inequality (4.17).

In conclusion, we have the following global regularity theorem.

Theorem 4.2 (Global regularity vs. finite-time blow up). *Consider the damped EMA system (1.1) with radial symmetry (2.1) and initial data (1.2) satisfying (2.2). In addition, suppose the potential satisfies $\phi_0''(r) < 1$ for all $r > 0$, corresponding to a non-vacuous initial density ρ_0 . The solution (ρ, \mathbf{u}, ϕ) develops a singular shock at a finite time T_c and location $r_c = r(T_c; r_0)$, namely*

$$(4.18) \quad \lim_{t \rightarrow T_*^-} \partial_r u(r_*, t) = -\infty, \quad \lim_{t \rightarrow T_*^-} \rho(r_*, t) = \infty,$$

if and only if there exists an $r > 0$ such that the following inequalities are met:

- *Strong damping* ($\beta > 2\sqrt{\kappa}$)

$$\left[-\frac{\lambda_1 u'_0(r) + \kappa \phi''_0(r)}{\kappa(1 - \phi''_0(r))} \right]^{\lambda_2} \geq \left[-\frac{\lambda_2 u'_0(r) + \kappa \phi''_0(r)}{\kappa(1 - \phi''_0(r))} \right]^{\lambda_1}, \quad \text{and}$$

$$\max \left\{ u'_0(r) + \lambda_2 \phi''_0(r), u'_0(r) + \lambda_1 \phi''_0(r) \right\} < 0,$$

where

$$\lambda_1 = \frac{\beta - \sqrt{\beta^2 - 4\kappa}}{2}, \quad \lambda_2 = \frac{\beta + \sqrt{\beta^2 - 4\kappa}}{2}.$$

- *Critical damping* ($\beta = 2\sqrt{\kappa}$).

$$\frac{u'_0(r)}{u'_0(r) + \alpha \phi''_0(r)} \leq \ln \left[-\frac{u'_0(r) + \alpha \phi''_0(r)}{\alpha(1 - \phi''_0(r))} \right], \quad \text{and}$$

$$\max \left\{ u'_0(r), u'_0(r) + \alpha \phi''_0(r) \right\} < 0,$$

where $\alpha = \frac{\beta}{2}$.

- *Weak damping* ($\beta < 2\sqrt{\kappa}$).

$$\left[\frac{u'_0(r) + \alpha \phi''_0(r)}{1 - \phi''_0(r)} \right]^2 + \left[\frac{\omega \phi''_0(r)}{1 - \phi''_0(r)} \right]^2 \geq \kappa e^{\beta t^*},$$

where

$$t^* = \frac{1}{\omega} \left[\beta_0 + \arctan \left(\frac{\omega u'_0(r)}{\alpha u'_0(r) + \kappa \phi''_0(r)} \right) \right], \quad \omega = \frac{1}{2} \sqrt{4\kappa - \beta^2}, \quad \alpha = \frac{\beta}{2},$$

$$\beta_0 = \begin{cases} 0, & \alpha u'_0(r) + \kappa \phi''_0(r) < 0 \text{ and } u'_0(r) < 0, \\ \pi, & \alpha u'_0(r) + \kappa \phi''_0(r) > 0, \\ 2\pi, & \alpha u'_0(r) + \kappa \phi''_0(r) < 0 \text{ and } u'_0(r) > 0. \end{cases}$$

Otherwise, ρ and $\nabla \mathbf{u}$ remain uniformly bounded for all time.

Proof. The proof utilizes the qualitative analysis of the spectral dynamics along characteristic paths, as established through the auxiliary variables $(w(t), s(t))$ and the local well-posedness results in Theorem 2.1.

For initial data (ρ_0, u_0, ϕ_0) satisfying the subcritical conditions, the auxiliary variable $s(t)$ remains strictly positive for all $t \geq 0$ along every characteristic path $X(t; r_0)$. Consequently, the quantities $p(t) = w(t)/s(t)$ and $\mu(t) = 1 - 1/s(t)$ remain uniformly bounded for all time.

By Lemma 3.2, the uniform boundedness of $p(\cdot, t)$ implies that $\|\nabla \mathbf{u}(\cdot, t)\|_{L^\infty} < \infty$ for all $t \geq 0$. Furthermore, utilizing the spectral representation of the density $\rho = (1 - \mu)(1 - \nu)^{n-1}$ and applying the bounds on $\|\nu(r, t)\|_{L^\infty}$ from Lemma 3.5, we conclude that $\|\rho(\cdot, t)\|_{L^\infty}$ is controlled by the uniform bounds on μ . Thus, global regularity of the damped EMA system follows from the regularity criterion (2.14).

Conversely, suppose the initial data is supercritical, satisfying the inequalities in Theorem 4.2 for some $r_0 > 0$. The corresponding trajectory in the (w, s) phase plane intersects the line $s = 0$ at a finite time T_c . As $t \rightarrow T_c^-$, we observe the following:

$$\lim_{t \rightarrow T_c^-} \mu(t) = 1 - \lim_{t \rightarrow T_c^-} \frac{1}{s(t)} = -\infty.$$

$$\lim_{t \rightarrow T_c^-} p(t) = \lim_{t \rightarrow T_c^-} \frac{s'(t)}{1 - s(t)} = - \lim_{t \rightarrow T_c^-} \left(\log((1 - s(t))) \right)' = -\infty.$$

This implies the ODE system (3.3) with initial data $p(0) = u'_0(r_0), \mu(0) = \phi''_0(r_0)$ becomes unbounded in finite time T_c at $r_c = r(T_c : r_0)$. In vacuum states, while the density remains zero, u_r satisfies the blow-up conditions defined in (2.16), completing the proof. \square

Remark 4.2. In the original analysis of the undamped EMA system [31], a necessary condition for global regularity was the density lower bound $\rho_0 \geq 2^{-n}$, where n is the dimension. This restriction is derived from the threshold condition $|u'_0(r)| < \sqrt{\kappa(1 - 2\phi''_0(r))}$, which implicitly requires the potential to satisfy $\phi''_0(r) \leq 1/2$. Given the spectral representation of the density $\rho = (1 - \phi'')(1 - \phi'/r)^{n-1}$, they obtained the aforementioned lower bound on ρ_0 .

With the introduction of velocity damping, this density bound is effectively removed in the strong and critical damping regimes. Our results demonstrate that for $\beta \geq 2\sqrt{\kappa}$, the system admits globally regular solutions for initial density that are arbitrarily small, and as established in Theorem 4.1, regularity can even persist in the vacuous state $\rho_0 = 0$. For example, in Theorem 4.2, when $\beta \geq 2\sqrt{\kappa}$, the condition $u'_0(r) \geq \phi''_0(r)\beta/2$ alone suffices to guarantee global regularity.

In contrast, this relaxation does not extend to the weakly damped regime. As we readily observe from rearranging the supercritical threshold inequality (4.17), we find that regularity requires:

$$1 - \mu_0 > \left[\frac{(u'_0(r) + \alpha\phi''_0(r))^2 + (\omega\phi''_0(r))^2}{\kappa e^{2\alpha t^*}} \right]^{1/2},$$

and similar bounds hold for ν :

$$1 - \nu_0 > \left[\frac{(u_0(r) + \alpha\phi'_0(r))^2 + (\omega\phi'_0(r))^2}{\kappa r^2 e^{2\alpha t^*}} \right]^{1/2}.$$

As $\rho = (1 - \mu)(1 - \nu)^{n-1}$, we derive a necessary density lower bound for global regularity:

$$(4.19) \quad \rho_0 > \left[\frac{(u'_0(r) + \alpha\phi''_0(r))^2 + (\omega\phi''_0(r))^2}{\kappa e^{2\alpha t^*}} \right]^{1/2} \left[\frac{(u_0(r) + \alpha\phi'_0(r))^2 + (\omega\phi'_0(r))^2}{\kappa r^2 e^{2\alpha t^*}} \right]^{n/2}$$

In other words, in the weakly damped regime, the density cannot be too low for any initial data to maintain global regularity. This further supports the universal finite time blow-up result for the vacuous state presented in the weakly damped regime in theorem 4.1.

Remark 4.3. Furthermore, we observe that the restriction $s_0 > 0$, or equivalently $1 - \mu_0 > 0$, is a natural requirement for the existence of smooth solutions. The explicit phase plane analysis indicates that any trajectory originating from non-positive initial data ($s_0 \leq 0$) will, by the Intermediate Value Theorem, either originate in a singular state or cross the $s = 0$ axis in finite time, resulting in finite-time singularity formation. Consequently, this assumption does not limit the scope of our global regularity results.

Remark 4.4. As noted earlier, the damped EMA system reduces to the damped Euler-Poisson system in one dimension. The critical thresholds for this 1D case were previously established in [3]. Our results in Theorem 4.2 are consistent with this prior work under their assumptions and recover their thresholds.

4.4. Large-time behavior. The utility of the auxiliary dynamics for $(w(t), s(t))$ extends beyond the characterization of critical thresholds. The explicit solutions for these quantities also determine the rate at which the system relaxes toward the equilibrium state. Given the transformation $(p, \mu) = (\frac{w}{s}, \frac{s-1}{s})$, it follows that for any subcritical initial data, where $s(t) > 0$ for all time $t \geq 0$, the convergence of (p, u) to $(0, 0)$ is determined by the decay rate of $(w(t), s(t) - 1)$. Specifically, we will study the large-time behavior of the following quantities:

$$(p(r, t), q(r, t), \mu(r, t), \nu(r, t)) = \left(\partial_r u(r, t), \frac{u(r, t)}{r}, \partial_r^2 \phi(r, t), \frac{\partial_r \phi(r, t)}{r} \right).$$

Recall the notation $A \lesssim B$ means $A \leq CB$ for some positive constant C which depends on up to parameters β, κ , dimension n , the initial data and in the case of critically damped regime, some small $\varepsilon > 0$.

Remark 4.5. It's important to emphasize that while the primary focus of our phase plane analysis is the pair (p, μ) , the tangential quantities (q, ν) satisfy the exact same underlying dynamics as (3.3). Because the evolution of these spectral components is identical, all conclusions derived for (p, μ) , particularly those regarding the large-time asymptotic behavior and the exponential rate of decay, extend directly to (q, ν) as well.

- *Strong damping* ($\beta > 2\sqrt{\kappa}$). From (4.8a) and (4.8b), we obtain the following large time behavior of $(w(t), s(t))$

$$|w(t), s(t) - 1| \lesssim \begin{cases} e^{-\lambda_1 t}, & \text{if } A \neq 0, \\ e^{-\lambda_2 t}, & \text{if } A = 0, \end{cases}$$

This implies

$$\|p(\cdot, t), \mu(\cdot, t)\|_{L^\infty} \lesssim \begin{cases} e^{-\lambda_1 t}, & \text{if } \frac{p_0 + \lambda_2 \mu_0}{1 - \mu_0} \neq 0, \\ e^{-\lambda_2 t}, & \text{if } \frac{p_0 + \lambda_2 \mu_0}{1 - \mu_0} = 0. \end{cases}$$

In addition, from Remark 4.5 we realize that the above decay rate also applies to (q, ν) :

$$\|p(\cdot, t), \mu(\cdot, t), q(\cdot, t), \nu(\cdot, t)\|_{L^\infty} \lesssim \begin{cases} e^{-\lambda_1 t}, & \text{if } \frac{p_0 + \lambda_2 \mu_0}{1 - \mu_0} \neq 0, \\ e^{-\lambda_2 t}, & \text{if } \frac{p_0 + \lambda_2 \mu_0}{1 - \mu_0} = 0. \end{cases}$$

Next, we investigate the asymptotic behavior of ρ . From the spectral representation of ρ (3.6), we get

$$\rho = (1 - \nu)^{n-1} (1 - \mu) = 1 - \mu - (n-1)\nu + R(\mu, \nu),$$

where the remainder term R consists of all higher order terms of μ and ν . This implies the rate at which ρ approaches 1 is determined by the decay rate of μ and ν . We then readily observe

$$\|\rho(\cdot, t) - 1\|_{L^\infty} \lesssim \begin{cases} e^{-\lambda_1 t}, & \text{if } \frac{u'_0(r) + \lambda_2 \phi''_0(r)}{1 - \phi''_0(r)} \neq 0, \\ e^{-\lambda_2 t}, & \text{if } \frac{u'_0(r) + \lambda_2 \phi''_0(r)}{1 - \phi''_0(r)} = 0. \end{cases}$$

Similarly, from the decay of $(\mu(\cdot, t), \nu(\cdot, t))$ we conclude

$$\|\partial_r^2 \phi(\cdot, t), \partial_r \phi(\cdot, r)\|_{L^\infty} \lesssim \begin{cases} e^{-\lambda_1 t}, & \text{if } \frac{u'_0(r) + \lambda_2 \phi''_0(r)}{1 - \phi''_0(r)} \neq 0, \\ e^{-\lambda_2 t}, & \text{if } \frac{u'_0(r) + \lambda_2 \phi''_0(r)}{1 - \phi''_0(r)} = 0. \end{cases}$$

In summary, the large time asymptotic behavior of the system is given as

$$(4.20) \quad \|\nabla \mathbf{u}(\cdot, t), \mathbf{u}(\cdot, t), \rho(\cdot, t) - 1, \partial_r^2 \phi(\cdot, t), \partial_r \phi(\cdot, t)\|_{L^\infty} \lesssim \begin{cases} e^{-\lambda_1 t}, & \text{if } \frac{u'_0(r) + \lambda_2 \phi''_0(r)}{1 - \phi''_0(r)} \neq 0, \\ e^{-\lambda_2 t}, & \text{if } \frac{u'_0(r) + \lambda_2 \phi''_0(r)}{1 - \phi''_0(r)} = 0, \end{cases}$$

- *Critical damping* ($\beta = 2\sqrt{\kappa}$). Following the same argument, we observe

$$|s(t) - 1, w(t)| \lesssim \begin{cases} te^{-\alpha t}, & \text{if } w_0 + \alpha(s_0 - 1) \neq 0, \\ e^{-\alpha t}, & \text{if } w_0 + \alpha(s_0 - 1) = 0, \end{cases}$$

It's clear that $te^{-\alpha t}$ still exhibits the asymptotic exponential decay rate of $-\alpha$,

$$te^{-\alpha t} = e^{-\alpha t(1 - \frac{\ln t}{\alpha t})} \xrightarrow{t \rightarrow \infty} e^{-\alpha t}.$$

To ensure uniform boundedness in time, we let $\varepsilon > 0$ be arbitrarily small, and use $t \leq \frac{1}{\varepsilon} e^{\varepsilon t}$ to derive

$$|s(t) - 1, w(t)| \lesssim e^{-(\alpha - \varepsilon)t}, \quad \text{if } w_0 + \alpha(s_0 - 1) \neq 0.$$

This implies

$$(4.21) \quad \|\nabla \mathbf{u}(\cdot, t), \mathbf{u}(\cdot, t), \rho(\cdot, t) - 1, \partial_r^2 \phi(\cdot, t), \partial_r \phi(\cdot, t)\|_{L^\infty} \lesssim \begin{cases} e^{-(\alpha - \varepsilon)t}, & \text{if } \frac{u'_0(r) + \alpha \phi''_0(r)}{1 - \phi''_0(r)} \neq 0, \\ e^{-\alpha t}, & \text{if } \frac{u'_0(r) + \alpha \phi''_0(r)}{1 - \phi''_0(r)} = 0. \end{cases}$$

- *Weak damping* ($\beta < 2\sqrt{\kappa}$). The oscillatory solutions (4.14a) and (4.14b) decay according to the real part, which gives

$$|s(t) - 1, w(s)| \lesssim e^{-\alpha t}.$$

Following our earlier discussion, this implies

$$(4.22) \quad \|\nabla \mathbf{u}(\cdot, t), \mathbf{u}(\cdot, t), \rho(\cdot, t) - 1, \partial_r^2 \phi(\cdot, t), \partial_r \phi(\cdot, t)\|_{L^\infty} \lesssim e^{-\alpha t}.$$

The following theorem summarizes the exponential decay rates for the damped EMA system (1.1) across all damping regimes.

Theorem 4.3. *Let (ρ, \mathbf{u}, ϕ) be a global classical solution to the damped EMA system (1.1) with radial symmetry. Let $\varepsilon > 0$ be arbitrary. Then, the solution converges to the equilibrium state $(\rho, \mathbf{u}) = (1, \mathbf{0})$ at an exponential rate:*

$$(4.23) \quad \|\nabla \mathbf{u}(\cdot, t), \mathbf{u}(\cdot, t), \rho(\cdot, t) - 1, \partial_r^2 \phi(\cdot, t), \partial_r \phi(\cdot, t)\|_{L^\infty} \lesssim e^{-\gamma t},$$

where the decay constant γ is determined by the damping coefficient β and the initial condition:

- *Strong damping* ($\beta > 2\sqrt{\kappa}$).

$$\gamma = \begin{cases} \frac{\beta - \sqrt{\beta^2 - 4\kappa}}{2}, & \text{if } \frac{u'_0(r) + \lambda_2 \phi''_0(r)}{1 - \phi''_0(r)} \neq 0, \\ \frac{\beta + \sqrt{\beta^2 - 4\kappa}}{2} & \text{if } \frac{u'_0(r) + \lambda_2 \phi''_0(r)}{1 - \phi''_0(r)} = 0. \end{cases}$$

- *Critical damping* ($\beta = 2\sqrt{\kappa}$).

$$\gamma = \begin{cases} \frac{\beta}{2} - \varepsilon, & \text{if } \frac{u'_0(r) + \alpha \phi''_0(r)}{1 - \phi''_0(r)} \neq 0, \\ \frac{\beta}{2}, & \text{if } \frac{u'_0(r) + \alpha \phi''_0(r)}{1 - \phi''_0(r)} = 0. \end{cases}$$

- *Weak damping* ($\beta < 2\sqrt{\kappa}$).

$$\gamma = \frac{\beta}{2}.$$

Remark 4.6. The quantitative results established in Theorem 4.3 may offer a complementary perspective to the geometric framework introduced by G. Loeper [25]. In the original derivation, the Euler–Monge–Ampère system is presented as a canonical relaxation of geodesics on the group of volume-preserving diffeomorphisms $\mathcal{D}_\mu(\Omega)$ of the domain Ω . However, for unprepared initial data, such approximate geodesics are prone to persistent, high-frequency oscillations, leading to weak convergence results in the quasi-neutral limit. Although our analysis is restricted to the radially symmetric setting on \mathbb{R}^n while Loeper’s work was posed on the torus \mathbb{T}^n , the result raises the question of whether the incorporation of linear damping could stabilize the quasi-neutral convergence.

5. A LYAPUNOV FUNCTION BASED APPROACH TO CRITICAL THRESHOLDS

In this section, we provide an alternative construction of the critical threshold, represented as part of the solution trajectory to the system (4.4) satisfying certain properties. Let C be a trajectory of (4.4) starting at $(0, 0)$ and traces backwards in negative time, and let the region R_1 be defined as $R_1 := \{(w, s) : w < 0, s > 0\}$.

- (I) If $\beta \geq 2\sqrt{\kappa}$, then the trajectory C will not exit the region R_1 (see explicit expressions of C in (5.1), (5.3), and discussions in Lemma 5.1). We define the subcritical region Σ_b to be the open set in $\mathbb{R} \times \mathbb{R}_+$ to the right of the curve C .
- (II) If $\beta < 2\sqrt{\kappa}$, the trajectory C will exit the region R_1 at $(0, s^*)$, where the value of s^* is specified in (5.7). Let C_* denote the continuation of C that starting at $(0, s^*)$ and intersects $\{s = 0\}$ at $(w^*, 0)$. We define the subcritical region Σ_b to be the open set enclosed by $C \cup C_*$ and $\{s = 0\}$.

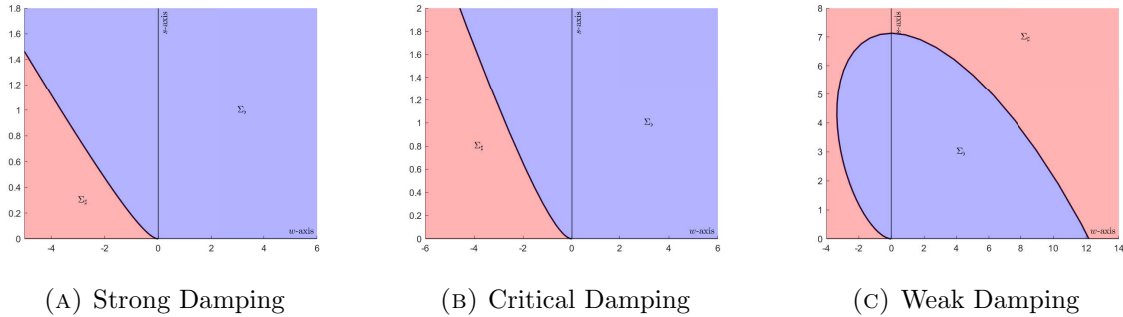


FIGURE 1. Phase portraits of the critical thresholds for the three damping regimes.

Solving for (4.4) explicitly yields the following representations of C :

- (I) *Strong damping* ($\beta > 2\sqrt{\kappa}$). The solutions $(w(t), s(t))$ are given as

$$(5.1a) \quad s(t) = -\frac{\lambda_2}{\lambda_2 - \lambda_1} e^{-\lambda_1 t} + \frac{\lambda_1}{\lambda_2 - \lambda_1} e^{-\lambda_2 t} + 1,$$

$$(5.1b) \quad w(t) = \frac{\lambda_1 \lambda_2}{\lambda_2 - \lambda_1} (e^{-\lambda_1 t} - e^{-\lambda_2 t}),$$

where

$$\lambda_1 = \frac{\beta - \sqrt{\beta^2 - 4\kappa}}{2}, \quad \lambda_2 = \frac{\beta + \sqrt{\beta^2 - 4\kappa}}{2}.$$

Let C_s be a portion of this trajectory defined as

$$(5.2) \quad C_s := \left\{ (w(t), s(t)) : t \in (-\infty, 0], (w(0), s(0)) = (0, 0) \right\}.$$

(II) *Critical damping* ($\beta = 2\sqrt{\kappa}$). The solution $(w(t), s(t))$ is given as

$$(5.3a) \quad s(t) = -e^{-\alpha t} - \alpha t e^{-\alpha t} + 1,$$

$$(5.3b) \quad w(t) = \alpha^2 t e^{-\alpha t}.$$

Here $\alpha = \beta/2$. Let C_c be a portion of this trajectory defined as

$$(5.4) \quad C_c := \left\{ (w(t), s(t)) : t \in (-\infty, 0], (w(0), s(0)) = (0, 0) \right\}.$$

(III) *Weak damping* ($\beta < 2\sqrt{\kappa}$). The Solution $(w(t), s(t))$ is given as

$$(5.5a) \quad s(t) = \left[-\cos(\omega t) - \frac{\alpha}{\omega} \sin(\omega t) \right] e^{-\alpha t} + 1,$$

$$(5.5b) \quad w(t) = e^{-\alpha t} \left(\frac{\kappa}{\omega} \right) \sin(\omega t).$$

Here $\omega = \frac{1}{2}\sqrt{4\kappa - \beta^2}$. Let $\tau := \sup\{t < 0 : s(t) = 0\}$ be the first negative time at which $s(\tau) = 0$. Let C_w be a portion of this trajectory defined as

$$(5.6) \quad C_w := \left\{ (w(t), s(t)) : t \in [\tau, 0], (w(0), s(0)) = (0, 0) \right\}.$$

The trajectories C_s, C_c and C_w constructed above define the critical threshold curves for their respective damping regimes. A more precise construction of the super- and subcritical regions utilizing the comparison principles will be provided. Note that the critical threshold in our case is *sharp*, hence the supercritical region Σ_{\sharp} is taken to be the complement of the subcritical regions, i.e., $\Sigma_{\sharp} := \mathbb{R} \times \mathbb{R}_+ \setminus \Sigma_{\flat}$.

Remark 5.1. In the construction of subcritical regions for the weakly damped regime, the union $C \cup C_*$ corresponds precisely to the solution trajectory C_w defined in (5.6). The region Σ_{\flat} is well-defined as the trajectory of (4.4) is expanding when traced in negative time. Since $(w^*, 0)$ represents the intersection of C_w with $\{s = 0\}$ at the first negative time, it follows that $w^* > 0$.

Remark 5.2. This construction follows from the observation that each integral curve in the phase plane either remains in the region $\{s > 0\}$ for all time, or else reaches the boundary $\{s = 0\}$ at some finite time $t_* > 0$.

In the latter case, the intersection with $\{s = 0\}$ can occur transversely or tangentially. If the curve touches $\{s = 0\}$ tangentially at some time t_* , then $s(t_*) = 0$ and $s'(t_*) = 0$. By (4.4), this can happen only at $(w, s) = (0, 0)$. Consequently, Poincaré's uniqueness theorem for autonomous systems implies that distinct integral curves cannot intersect. Hence, the trajectory through $(0, 0)$ partitions the family of integral curves of (4.4) into those that remain in $\{s > 0\}$ and those that intersect $\{s = 0\}$. The following figure depicts the phase plane velocity field and three distinct integral curves.

Next, we prove a lemma that verifies the claim made in the construction of the critical threshold.

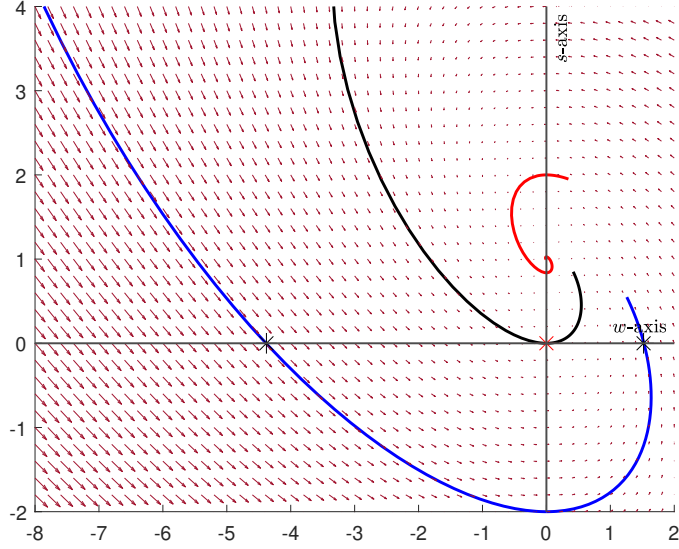


FIGURE 2. Illustration of the vector field.

Lemma 5.1. *Let $\beta \geq 2\sqrt{\kappa}$. Then the solution trajectories to the system (4.4), traced backwards in negative from the initial data*

$$w(0) = 0, \quad s(0) = 0,$$

remained confined within the region $R_1 = \{(w, s) : w < 0, s > 0\}$ for all time $t < 0$. In other words, $C_s \subset R_1$ and $C_b \subset R_1$.

Proof. Consider the case $\beta > 2\sqrt{\kappa}$, where solution trajectory is given by (5.1). We first observe the asymptotic behavior

$$\lim_{t \rightarrow -\infty} s(t) = \infty, \quad \lim_{t \rightarrow -\infty} w(t) = -\infty.$$

In addition, we note that $s(t)$ and $w(t)$ both have at most one local extremum. Since $s'(0) = w(0) = 0$, this extremum for $s(t)$ is achieved, implying $s(t)$ is monotone increasing for all $t < 0$. For $w(t)$, we compute its critical point

$$w'(t) = \frac{\lambda_1 \lambda_2}{\lambda_2 - \lambda_1} \left(-\lambda_1 e^{-\lambda_1 t} + \lambda_2 e^{-\lambda_2 t} \right).$$

Equating $w'(t)$ to 0 and solve for t to obtain

$$t = \frac{1}{\lambda_2 - \lambda_1} \ln \left(\frac{\lambda_2}{\lambda_1} \right) > 0.$$

Hence we see that $w(t)$ is monotone decreasing for all $t < 0$. Hence $C_s \subset R_1$. Similarly, we conclude $C_b \subset R_1$. \square

The quantity s^* which defines the point of intersection earlier and the domains of the Lyapunov functions (5.8) and (5.11) introduced below is determined from explicitly calculating

the s -axis intercept of the solution trajectory for the weakly damped system (4.4). We solve for the first negative time t^* at which $w(t^*) = 0$. To this end, we compute

$$e^{-\alpha t^*} \frac{2\kappa}{\sqrt{4\kappa - \beta^2}} \sin(\omega t^*) = 0 \iff \sin(\omega t^*) = 0.$$

It's then straightforward to verify that $t^* = -\frac{\pi}{\omega}$. Hence we obtain

$$(5.7) \quad s(t^*) = \left(-\cos(-\pi) - \frac{\beta}{\sqrt{4\kappa - \beta^2}} \sin(-\pi) \right) e^{\frac{\alpha\pi}{\omega}} + 1 = e^{\frac{\beta\pi}{\sqrt{4\kappa - \beta^2}}} + 1.$$

For analytical purpose, it is desirable to represent the critical threshold curve C as a level set of suitable scalar functions of (w, s) . Especially in the undamped case $\beta = 0$, the trajectories coincide with the level curves of the function (4.5). To express the solution trajectories and the threshold regions more succinctly, we construct the following Lyapunov functions, based on the approach utilized in [31]. This idea was first adopted in [3] for the damped Euler-Poisson equations, and later extended to [12] and [26]. Let us introduce the first such Lyapunov function,

$$(5.8) \quad \mathcal{L}_P(w, s) = w + \sqrt{2P(s)},$$

where the function $P(s)$ satisfies the following ODE

$$(5.9) \quad \frac{dP}{ds} = \beta\sqrt{2P(s)} + \kappa(1 - s), \quad P(0) = 0.$$

The next theorem precisely characterizes the relationship between the level sets of the above Lyapunov function and the solution trajectories to the system (4.4).

Theorem 5.2. *Suppose $\mathcal{L}_P(w, s)$ and $P(s)$ satisfy (5.8) and (5.9), respectively, and*

$$\text{Range}\{s(t) : t \in I\} \subset \text{Dom}(P).$$

Let $(w(t), s(t))$ be a solution to (4.4) for all $t \in I$. If $\mathcal{L}_P(w(t_0), s(t_0)) = 0$ for some $t_0 \in I$, then the following holds:

$$\mathcal{L}_P(w(t), s(t)) = 0, \quad \forall t \in I.$$

Proof. We differentiate $\mathcal{L}_P(w, s)$ with respect to time and compute

$$\begin{aligned} \frac{d}{dt} \mathcal{L}_P(w(t), s(t)) &= w'(t) + \frac{1}{\sqrt{2P(s(t))}} \cdot \frac{dP}{ds} \cdot s'(t) \\ &= \kappa(1 - s(t)) - \beta w(t) + \frac{1}{\sqrt{2P(s(t))}} \left(\beta\sqrt{2P(s(t))} + \kappa(1 - s(t)) \right) \cdot w(t) \\ &= \kappa(1 - s(t)) + \frac{\kappa(1 - s(t))}{\sqrt{2P(s(t))}} w(t) \\ &= \frac{\kappa(1 - s(t))}{\sqrt{2P(s(t))}} \mathcal{L}_P(w(t), s(t)). \end{aligned}$$

Consequently, we obtain

$$(5.10) \quad \mathcal{L}_P(w(t), s(t)) = \mathcal{L}_P(w(t_0), s(t_0)) \exp \left(\int_{t_0}^t \frac{\kappa(1 - s(\tau))}{\sqrt{2P(s(\tau))}} d\tau \right) = 0.$$

□

It follows from the Theorem 5.2 that the condition $P(0) = 0$ is specified so that the zero level set of $\mathcal{L}_P(w, s)$ represent the solution trajectory to (4.4) passing through $(0, 0)$ in the region $R_1 := \{(w, s) : w < 0, s > 0\}$. In the case of weak damping, the solution trajectory C_w will exit the region R_1 at $(0, s^*)$. For expression of s^* , see (5.7). To represent the part of C_w in the region $R_2 := \{(w, s) : w > 0, s > 0\}$, we construct an additional Lyapunov function, which satisfies the same property as stated in Theorem 5.2,

$$(5.11) \quad \mathcal{L}_N(w, s) = w - \sqrt{2N(s)},$$

where the function $N(s)$ satisfies the ODE

$$(5.12) \quad \frac{dN}{ds} = -\beta\sqrt{2N(s)} + \kappa(1 - s), \quad N(s^*) = 0, \quad s^* = e^{\frac{k\pi}{\sqrt{4 - k^2}}} + 1.$$

A similar relation to (5.10) holds for \mathcal{L}_N :

$$(5.13) \quad \mathcal{L}_N(w(t), s(t)) = \mathcal{L}_N(w(t_0), s(t_0)) \exp\left(\int_{t_0}^t \frac{\kappa(s(\tau) - 1)}{\sqrt{2N(s(\tau))}} d\tau\right).$$

The choice of s^* ensures that the union of sets $\{\mathcal{L}_p(w, s) = 0\}$ and $\{\mathcal{L}_N(w, s) = 0\}$ constitutes the single solution trajectory defined in (5.6).

Next, we present a version of the comparison principle based on the Lyapunov functions (5.8) and (5.11), as a corollary from 5.2.

Proposition 5.3 (Comparison principles). *Let $(w(t), s(t))$ be a solution to the system (4.4). Denote by C the solution trajectory over the time interval (t_0, t_1) , namely*

$$C := \{(w(t), s(t)) : t \in (t_0, t_1)\}.$$

Then the following results hold:

- Let $R_1 = \{(w, s) : w < 0, s > 0\}$ and suppose $C \subset R_1$, then

$$(5.14) \quad \mathcal{L}_P(w(t_0), s(t_0)) \leq 0 \iff \mathcal{L}_P(w(t), s(t)) \leq 0, \quad \forall t \in [t_0, t_1].$$

In addition,

$$(5.15) \quad \mathcal{L}_P(w(t_0), s(t_0)) > 0 \iff \mathcal{L}_P(w(t_1), s(t_1)) > 0, \quad \forall t \in [t_0, t_1].$$

- Let $R_2 = \{(w, s) : w > 0, s > 0\}$ and suppose $C \subset R_2$, then

$$(5.16) \quad \mathcal{L}_N(w(t_0), s(t_0)) < 0 \iff \mathcal{L}_N(w(t_1), s(t_1)) < 0, \quad \forall t \in [t_0, t_1].$$

In addition,

$$(5.17) \quad \mathcal{L}_N(w(t_0), s(t_0)) \geq 0 \iff \mathcal{L}_N(w(t_1), s(t_1)) \geq 0, \quad \forall t \in [t_0, t_1].$$

Proof. It suffices to establish the strict inequalities, as the non-strict cases follow directly from the integral representation (5.10). While we could control the integral in the exponential term in (5.10) by following the approach in [12, Proposition 4.7], the result is an immediate consequence of the uniqueness theorem for autonomous ODE system.

Let \mathcal{C}_0 denote the zero level set of $\mathcal{L}_P(w(t), s(t))$, which represents the unique solution trajectory of (4.4) passing through the origin. Consider an arbitrary trajectory \mathcal{C} starting at $(w(t_0), s(t_0))$ such that $\mathcal{L}_P(w(t_0), s(t_0)) \neq 0$. Since \mathcal{C} and \mathcal{C}_0 are distinct integral curves of an autonomous system, they must be disjoint for all time. Consequently, $\mathcal{L}_P(w(t), s(t))$ can never vanish. The analogous strict inequality for \mathcal{L}_N follows by the same argument. \square

Next, we utilize the above comparison principles to give precise construction and characterization of the super- and subcritical regions.

(I) In the region $R_1 = \{(w, s) : w < 0, s > 0\}$, let C_1 be a trajectory of (4.4) that passes through $(0, 0)$, which can be represented as the level set $\mathcal{L}_p(w, s) = 0$ by Theorem 5.2. We claim the lifespan of $P(s)$ is given as follows,

$$(5.18) \quad \text{Dom}(P) = \begin{cases} [0, \infty) & \beta \geq 2\sqrt{\kappa}, \\ [0, s^*] & 0 < \beta < 2\sqrt{\kappa}. \end{cases}$$

The claim follows directly from Lemma 5.1. Depending on the damping regime, there are two situations:

(1) If $\beta \geq 2\sqrt{\kappa}$, C_1 won't exit the region R_1 and can be represented as $\{(w, s) : w = -\sqrt{2P(s)}, s \in [0, \infty)\}$. In this case, the subcritical region is characterized as

$$\Sigma_b = \{(w, s) : w > -\sqrt{2P(s)}, s > 0\}.$$

Namely, the region Σ_b consists of the open set in $\mathbb{R} \times \mathbb{R}_+$ to the right of the curve C_1 . The supercritical region Σ_\sharp is defined to be $(\mathbb{R} \times \mathbb{R}_+) \setminus \Sigma_b$, namely:

$$\Sigma_\sharp = \{(w, s) : w \leq -\sqrt{2P(s)}, s > 0\}.$$

The initial condition of P is chosen so that $\mathcal{L}_P(0, 0) = \sqrt{2P(0)} = 0$.

(2) If $\beta < 2\sqrt{\kappa}$, C_1 exits the region at $(0, s^*)$, and can be represented as $\{(w, s) : w = -\sqrt{2P(s)}, s \in [0, s^*]\}$. We continue our construction.

(II) In the region $R_2 = \{(w, s) : w > 0, s > 0\}$, let C_2 be a trajectory of (4.4) that passes through $(0, s^*)$. The lifespan of $N(s)$ is

$$(5.19) \quad \text{Dom}(N) = [0, s^*].$$

The trajectory takes the form $C_2 = \{(w, s) : w = \sqrt{2N(s)}, s \in [0, s^*]\}$, and it exits the region at $(w^*, 0)$. In this case, the subcritical region is given as

$$\Sigma_b = \{(w, s) : \sqrt{2N(s)} > w > -\sqrt{2P(s)}, s \in (0, s^*)\}.$$

Namely, the region Σ_b consists of the open set in $\mathbb{R} \times \mathbb{R}_+$ bounded by the curve $C_1 \cup C_2$. The supercritical region Σ_\sharp is defined to be $(\mathbb{R} \times \mathbb{R}_+) \setminus \Sigma_b$. The initial condition of N is chosen so that $\mathcal{L}_N(0, s^*) = -\sqrt{2N(s^*)} = 0$.

Remark 5.3. To verify that the constructed set Σ_b is *invariant* in the sense of 4.2, we must show that any solution trajectory initialized within Σ_b never escapes. We focus on the weak damping case ($\beta < 2\sqrt{\kappa}$), as it includes the case when $\beta \geq 2\sqrt{\kappa}$.

The strict comparison principles established in Proposition 5.3 ensure that a trajectory cannot cross the lateral boundaries defined by the level sets $\mathcal{L}_P(w, s) = 0$ and $\mathcal{L}_N(w, s) = 0$. Thus, the only potential exit is through the bottom boundary segment $\{(w, 0) : 0 < w \leq w^*\}$. However, on this segment, the vertical velocity of the flow is given by $s'(t) = w(t) > 0$. This implies that the vector field points strictly *into* the region $s > 0$.

The comparison principle based approach yields another *sharp* characterization of the critical thresholds.

Theorem 5.4 (Global regularity). *Let (ρ, \mathbf{u}, ϕ) be a classical solution of the damped EMA system (1.1) with radial symmetry (2.1). Suppose that the initial data (\mathbf{u}_0, ϕ_0) lie within the following subcritical region:*

- *Strong or critical damping* ($\beta \geq 2\sqrt{\kappa}$):

$$(5.20) \quad u'_0(r) > (\phi''_0(r) - 1) \sqrt{2P\left(\frac{1}{1 - \phi''_0(r)}\right)}.$$

- *Weak damping* ($\beta < 2\sqrt{\kappa}$):

$$(5.21) \quad (1 - \phi''_0(r)) \sqrt{2N\left(\frac{1}{1 - \phi''_0(r)}\right)} > u'_0(r) > (\phi''_0(r) - 1) \sqrt{2P\left(\frac{1}{1 - \phi''_0(r)}\right)},$$

for all $r > 0$, then ρ and $\nabla \mathbf{u}$ are uniformly bounded in all time. Otherwise, suppose there exists an $r > 0$ such that either (5.20) or (5.21) is violated in their respective damping regimes. Then there exist a location r_c and a finite time T_c at which

$$(5.22) \quad \lim_{t \rightarrow T_c^-} \partial_r u(r_c, t) = -\infty, \quad \lim_{t \rightarrow T_c^-} \rho(r_c, t) = \infty.$$

Proof. The global regularity is a direct consequence of the invariance of the subcritical region Σ_b . As established previously, any trajectory initialized within Σ_b remains confined to this set for all $t > 0$. Consequently, by invoking the same arguments utilized in the proof of Theorem 4.2, we obtain global regularity.

Conversely, for data in the supercritical region, the finite-time blowup scenario follows from a phase plane analysis argument. One can follow the approaches highlighted in either [12, Proposition 4.1] or [26, Proposition 4.5] almost verbatim. This completes the proof. \square

Remark 5.4. Let us recover the critical threshold for the undamped EMA system with radial symmetry using Theorem 5.4. Recall that this condition is given as

$$|u'_0(r)| < \sqrt{\kappa(1 - 2\phi''_0(r))}.$$

In the absence of damping ($\beta = 0$), The Lyapunov function takes the form $\mathcal{L}(w, s) = w^2 + \kappa(1 - s)^2$. As verified earlier, $\frac{d}{dt}\mathcal{L}(w, s) = 0$, implying that $w^2 + \kappa(1 - s)^2 = c$ for some constant c . Since the critical threshold curve crosses the origin $(0, 0)$ in the (w, s) -plane, we must have $c = \kappa$. This gives the explicit representation for both $P(s)$ and $N(s)$:

$$P(s) = N(s) = \frac{\kappa - \kappa(1 - s)^2}{2}.$$

Substituting $s = \frac{1}{1 - \phi''_0(r)}$ into both functions yields

$$P\left(\frac{1}{1 - \phi''_0(r)}\right) = N\left(\frac{1}{1 - \phi''_0(r)}\right) = \frac{\kappa(1 - 2\phi''_0(r))}{2(1 - \phi''_0(r))^2}.$$

Then using the subcritical condition (5.21) in Theorem 5.4, we obtain the critical threshold condition:

$$\sqrt{\kappa(1 - 2\phi''_0(r))} > u'_0(r) > -\sqrt{\kappa(1 - 2\phi''_0(r))}.$$

This recovers the critical threshold derived in [31].

APPENDIX A. LOCAL WELL-POSEDNESS AND REGULARITY CRITERION

Let $\Omega(\mathbf{x}, t)$ be a vector-valued radial function defined as

$$(A.1) \quad \Omega(\mathbf{x}, t) = \begin{bmatrix} p(|\mathbf{x}|, t) \\ q(|\mathbf{x}|, t) \\ \mu(|\mathbf{x}|, t) \\ \nu(|\mathbf{x}|, t) \end{bmatrix} = \begin{bmatrix} \partial_r u(r, t) \\ \frac{u(r, t)}{r} \\ \partial_r^2 \phi(r, t) \\ \frac{\partial_r \phi(r, t)}{r} \end{bmatrix}.$$

This allows us to compress the dynamics (3.11) and (3.14) into vector valued equation of Ω :

$$(A.2) \quad \partial_t \Omega + (\mathbf{u} \cdot \nabla) \Omega = \mathbf{F}(\Omega), \quad \mathbf{F}(\Omega) = \begin{bmatrix} -\Omega_1^2 - \kappa \Omega_3 - \beta \Omega_1 \\ -\Omega_2^2 - \kappa \Omega_4 - \beta \Omega_2 \\ \Omega_1(1 - \Omega_3) \\ \Omega_2(1 - \Omega_4) \end{bmatrix}.$$

Equivalently, we write

$$(A.3) \quad \partial_t \Omega_i + \nabla \cdot (\Omega_i \mathbf{u}) = \tilde{F}_i(\Omega), \quad i \in \{1, 2, 3, 4\}$$

where the forcing term \tilde{F}_i is defined as

$$(A.4) \quad \tilde{\mathbf{F}}(\Omega) := \mathbf{F}(\Omega) + (\nabla \cdot \mathbf{u}) \Omega = \begin{bmatrix} -\Omega_1^2 - \kappa \Omega_3 - \beta \Omega_1 + \Omega_1(\Omega_1 + (n-1)\Omega_2) \\ -\Omega_2^2 - \kappa \Omega_4 - \beta \Omega_2 + \Omega_2(\Omega_1 + (n-1)\Omega_2) \\ \Omega_1(1 - \Omega_3) + \Omega_3(\Omega_1 + (n-1)\Omega_2) \\ \Omega_2(1 - \Omega_4) + \Omega_4(\Omega_1 + (n-1)\Omega_2) \end{bmatrix}.$$

Here we used the relation

$$(A.5) \quad \nabla \cdot \mathbf{u} = p(r, t) + (n-1)q(r, t) = \Omega_1 + (n-1)\Omega_2.$$

We prove the Theorem 2.1.

Proof. Given any $s \geq 0$, we denote the fractional differential operator by $\Lambda^s := (-\Delta)^{\frac{s}{2}}$ and the homogeneous semi-norm by

$$\|f\|_{\dot{H}^s(\mathbb{R}^n)} = \|\Lambda^s f\|_{L^2(\mathbb{R}^n)}.$$

The notation \lesssim will be used throughout the proof, where $A \lesssim B$ means there exists a constant C , depending on the parameters and initial data, such that $A \leq CB$. In addition, we use ∂_j to denote $\frac{\partial}{\partial x_j}$. Let the energy $E_s(t)$ be defined as

$$E_s(t) := \frac{1}{2} \|\Omega\|_{H^s(\mathbb{R}^n)}^2 = \frac{1}{2} \|\Omega\|_{L^2(\mathbb{R}^n)}^2 + \frac{1}{2} \|\Lambda^s \Omega\|_{L^2(\mathbb{R}^n)}^2.$$

Next, we provide an a priori energy estimate. Let us first consider the L^2 energy estimate:

$$\begin{aligned} \frac{1}{2} \frac{d}{dt} \|\Omega\|_{L^2}^2 &= \sum_{i=1}^n \int_{\mathbb{R}^n} (\tilde{F}_i(\Omega) - \nabla \cdot (\Omega_i \mathbf{u})) \cdot \Omega_i \, dx \\ &= \sum_{i=1}^n \int_{\mathbb{R}^n} -\frac{1}{2} \Omega_i^2 (\nabla \cdot \mathbf{u}) + \tilde{F}_i(\Omega) \cdot \Omega_i \, dx \\ &\leq \sum_{i=1}^n \left(\|\nabla \cdot \mathbf{u}\|_{L^\infty} \|\Omega_i\|_{L^2}^2 + \|\tilde{F}_i(\Omega)\|_{L^2} \|\Omega_i\|_{L^2} \right) \end{aligned}$$

$$\begin{aligned}
&\leq \sum_{i=1}^n \left(\|\nabla \cdot \mathbf{u}\|_{L^\infty} \|\Omega_i\|_{L^2}^2 + (1 + \|\boldsymbol{\Omega}\|_{L^\infty}) \|\Omega_i\|_{L^2}^2 \right) \\
&\lesssim \left(1 + \|\nabla \cdot \mathbf{u}\|_{L^\infty} + \|\boldsymbol{\Omega}\|_{L^\infty} \right) \|\boldsymbol{\Omega}\|_{L^2}^2 \lesssim (1 + \|\boldsymbol{\Omega}\|_{L^\infty}) \|\boldsymbol{\Omega}\|_{L^2}^2.
\end{aligned}$$

Observe the quadratic dependence of \tilde{F}_i on $\boldsymbol{\Omega}$ leads to the following inequality:

$$\|\tilde{\mathbf{F}}(\boldsymbol{\Omega})\|_{L^2} \lesssim (1 + \|\boldsymbol{\Omega}\|_{L^\infty}) \|\boldsymbol{\Omega}\|_{L^2},$$

which is used in the third to last line. Next, we estimate the \dot{H}^s energy:

$$\begin{aligned}
\frac{1}{2} \frac{d}{dt} \|\Lambda^s \boldsymbol{\Omega}\|_{L^2}^2 &= \sum_{i=1}^n \int_{\mathbb{R}^n} \left[\Lambda^s \left(\tilde{F}_i(\boldsymbol{\Omega}) - \nabla \cdot (\Omega_i \mathbf{u}) \right) \right] \Lambda^s \Omega_i \, dx \\
&= - \sum_{i,j=1}^n \int_{\mathbb{R}^n} \left(\Lambda^s \partial_j (\Omega_i \cdot u_j) \cdot \Lambda^s \Omega_i \right) \, dx + \sum_{i=1}^n \int_{\mathbb{R}^n} \Lambda^s \tilde{F}_i(\boldsymbol{\Omega}) \cdot \Lambda^s \Omega_i \, dx \\
&= I + II.
\end{aligned}$$

Let us estimate I first. Observe

$$I = -\frac{1}{2} \sum_{i,j=1}^n \int_{\mathbb{R}^n} (\Lambda^s \Omega_i)^2 \cdot \partial_j u_j \, dx - \sum_{i,j=1}^n \int_{\mathbb{R}^n} [\Lambda^s \partial_j, u_j] \Omega_i \cdot \Lambda^s \Omega_i \, dx = I_1 + I_2.$$

where we use $[\cdot, \cdot]$ to denote the commutator, whose operation is given as

$$[\mathcal{J}, f]g = \mathcal{J}(fg) - f\mathcal{J}g.$$

For I_1 , we observe from (A.5) the following holds

$$\|\nabla \cdot \mathbf{u}\|_{L^\infty} \leq \|\Omega_1\|_{L^\infty} + (n-1) \|\Omega_2\|_{L^\infty} \lesssim \|\boldsymbol{\Omega}\|_{L^\infty}.$$

It then follows

$$I_1 = -\frac{1}{2} \sum_{i=1}^n \int_{\mathbb{R}^n} (\Lambda^s \Omega_i)^2 \nabla \cdot \mathbf{u} \, dx \leq \|\nabla \cdot \mathbf{u}\|_{L^\infty} \|\Lambda^s \Omega\|_{L^2}^2 \lesssim \|\boldsymbol{\Omega}\|_{L^\infty} \|\Lambda^s \Omega\|_{L^2}^2.$$

To estimate I_2 , we use a Kato-Ponce type commutator estimate,

$$\begin{aligned}
I_2 &\leq \sum_{i,j=1}^n \int_{\mathbb{R}^n} [\Lambda^s \partial_j, u_j] \Omega_i \cdot \Lambda^s \Omega_i \, dx \\
&\leq \sum_{i,j=1}^n \|[\Lambda^s \partial_j, u_j] \Omega_i\|_{L^2} \|\Lambda^s \Omega_i\|_{L^2} \\
&\lesssim \sum_{i,j=1}^n \left(\|\partial_j u_j\|_{L^\infty} \|\Lambda^s \Omega_i\|_{L^2} + \|\Lambda^s \partial_j u_j\|_{L^2} \|\Omega_i\|_{L^\infty} \right) \|\Lambda^s \Omega_i\|_{L^2} \\
&\lesssim \|\nabla \cdot \mathbf{u}\|_{L^\infty} \|\Lambda^s \boldsymbol{\Omega}\|_{L^2}^2 + \|\Lambda^s (\nabla \cdot \mathbf{u})\|_{L^2} \|\boldsymbol{\Omega}\|_{L^\infty} \|\Lambda^s \boldsymbol{\Omega}\|_{L^2} \\
&\lesssim \|\boldsymbol{\Omega}\|_{L^\infty} \|\Lambda^s \boldsymbol{\Omega}\|_{L^2}^2 + \|\Lambda^s (\nabla \cdot \mathbf{u})\|_{L^2} \|\boldsymbol{\Omega}\|_{L^\infty} \|\Lambda^s \boldsymbol{\Omega}\|_{L^2}.
\end{aligned}$$

We readily observe from (A.5) that the following holds:

$$\|\Lambda^s (\nabla \cdot \mathbf{u})\|_{L^2} \leq \|\Lambda^s \Omega_1\|_{L^2} + (n-1) \|\Lambda^s \Omega_2\|_{L^2} \lesssim \|\Lambda^s \boldsymbol{\Omega}\|_{L^2}.$$

Consequently,

$$I_2 \lesssim \|\boldsymbol{\Omega}\|_{L^\infty} \|\Lambda^s \boldsymbol{\Omega}\|_{L^2}^2.$$

Together the estimates of I_1 and I_2 give

$$(A.6) \quad I \lesssim \|\boldsymbol{\Omega}\|_{L^\infty} \|\Lambda^s \boldsymbol{\Omega}\|_{L^2}^2.$$

Let us estimate II . First observe the quadratic dependence of $\tilde{\mathbf{F}}$ on $\boldsymbol{\Omega}$ in (A.4) implies

$$\|\Lambda^s(\tilde{\mathbf{F}})(\boldsymbol{\Omega})\|_{L^2} \lesssim (1 + \|\boldsymbol{\Omega}\|_{L^\infty}) \|\Lambda^s \boldsymbol{\Omega}\|_{L^2}.$$

Hence, we obtain

$$(A.7) \quad \begin{aligned} II &= \sum_{i=1}^n \int_{\mathbb{R}^n} \Lambda^s \tilde{F}_i(\boldsymbol{\Omega}) \cdot \Lambda^s \Omega_i \, dx \\ &\leq \sum_{i=1}^n \|\Lambda^s \tilde{F}_i(\boldsymbol{\Omega})\|_{L^2} \|\Lambda^s \Omega_i\|_{L^2} \lesssim (1 + \|\boldsymbol{\Omega}\|_{L^\infty}) \|\Lambda^s \boldsymbol{\Omega}\|_{L^2}^2. \end{aligned}$$

Combining (A.6) and (A.7) to get

$$\frac{1}{2} \frac{d}{dt} \|\Lambda^s \boldsymbol{\Omega}\|_{L^2}^2 \lesssim (1 + \|\boldsymbol{\Omega}(\cdot, t)\|_{L^\infty}) \|\Lambda^s \boldsymbol{\Omega}\|_{L^2}^2.$$

Consequently, we have the following estimate on the energy $E_s(t)$:

$$(A.8) \quad \frac{d}{dt} E_s(t) \lesssim (1 + \|\boldsymbol{\Omega}(\cdot, t)\|_{L^\infty}) E_s(t).$$

If $s > \frac{n}{2}$, then Sobolev embedding gives local well-posedness and we apply Grönwall inequality to (A.8) to obtain

$$E_s(t) \leq E_s(0) \exp \left[C \int_0^T (1 + \|\boldsymbol{\Omega}(\cdot, t)\|_{L^\infty}) \, dt \right].$$

Hence, $E_s(t)$ is bounded as long as (2.15) holds. \square

REFERENCES

- [1] Vladimir Arnold. Sur la géométrie différentielle des groupes de lie de dimension infinie et ses applications à l'hydrodynamique des fluides parfaits. In *Annales de l'institut Fourier*, volume 16, pages 319–361, 1966.
- [2] Manas Bhatnagar and Hailiang Liu. Critical thresholds in 1D pressureless Euler–Poisson systems with variable background. *Physica D: Nonlinear Phenomena*, 414:132728, 2020.
- [3] Manas Bhatnagar and Hailiang Liu. Critical thresholds in one-dimensional damped Euler–Poisson systems. *Mathematical Models and Methods in Applied Sciences*, 30(05):891–916, 2020.
- [4] Manas Bhatnagar, Hailiang Liu, and Changhui Tan. Critical thresholds in the Euler–Poisson-alignment system. *Journal of Differential Equations*, 375:82–119, 2023.
- [5] Yann Brenier. Derivation of the Euler equations from a caricature of coulomb interaction. *Communications in Mathematical Physics*, 212(1):93–104, 2000.
- [6] Yann Brenier, Wilfrid Gangbo, Giuseppe Savaré, and Michael Westdickenberg. Sticky particle dynamics with interactions. *Journal de Mathématiques Pures et Appliquées*, 99(5):577–617, 2013.
- [7] Yann Brenier and Grégoire Loeper. A geometric approximation to the Euler equations: the Vlasov–Monge–Ampere system. *Geometric & Functional Analysis GAFA*, 14(6):1182–1218, 2004.
- [8] José A Carrillo, Young-Pil Choi, Dowan Koo, and Oliver Tse. Exponential and algebraic decay in Euler–alignment system with nonlocal interaction forces. *arXiv preprint arXiv:2510.14123*, 2025.
- [9] José A Carrillo, Young-Pil Choi, Eitan Tadmor, and Changhui Tan. Critical thresholds in 1D Euler equations with non-local forces. *Mathematical Models and Methods in Applied Sciences*, 26(01):185–206, 2016.
- [10] José A Carrillo and Sondre Galtung. Equivalence of entropy solutions and gradient flows for pressureless 1D Euler systemsuler systems. *arXiv preprint arXiv:2312.04932*, 2023.

- [11] José A Carrillo and Ruiwen Shu. Existence of radial global smooth solutions to the pressureless Euler–Poisson equations with quadratic confinement. *Archive for Rational Mechanics and Analysis*, 247(4):73, 2023.
- [12] Young-Pil Choi, Dong-ha Kim, Dowan Koo, and Eitan Tadmor. Critical thresholds in pressureless Euler–Poisson equations with background states. *Annales de l’Institut Henri Poincaré C*, 2025.
- [13] Tam Do, Alexander Kiselev, Lenya Ryzhik, and Changhui Tan. Global regularity for the fractional Euler alignment system. *Archive for Rational Mechanics and Analysis*, 228(1):1–37, 2018.
- [14] Shlomo Engelberg, Hailiang Liu, and Eitan Tadmor. Critical thresholds in Euler–Poisson equations. *Indiana University Mathematics Journal*, pages 109–157, 2001.
- [15] David Fajman, Maciej Maliborski, Maximilian Ofner, Todd Oliynyk, and Zoe Wyatt. A critical threshold for the cosmological Euler–Poisson system. *arXiv preprint arXiv:2512.19454*, 2025.
- [16] Wilfrid Gangbo, Truyen Nguyen, and Adrian Tudorascu. Euler–Poisson systems as action-minimizing paths in the Wasserstein space. *Archive for Rational Mechanics and Analysis*, 192(3):419–452, 2009.
- [17] Yan Guo. Smooth irrotational flows in the large to the Euler–Poisson system in \mathcal{R}^{3+1} . *Communications in Mathematical Physics*, 195:249–265, 1998.
- [18] Yan Guo, Lijia Han, and Jingjun Zhang. Absence of shocks for one dimensional Euler–Poisson system. *Archive for Rational Mechanics and Analysis*, 223(3):1057–1121, 2017.
- [19] Yan Guo and Benoit Pausader. Global smooth ion dynamics in the Euler–Poisson system. *Communications in Mathematical Physics*, 303:89–125, 2011.
- [20] Siming He and Eitan Tadmor. Global regularity of two-dimensional flocking hydrodynamics. *Comptes Rendus. Mathématique*, 355(7):795–805, 2017.
- [21] Alexandru D Ionescu and Benoit Pausader. The Euler–Poisson system in 2d: global stability of the constant equilibrium solution. *International Mathematics Research Notices*, 2013(4):761–826, 2013.
- [22] Juhi Jang. The two-dimensional Euler–Poisson system with spherical symmetry. *Journal of mathematical physics*, 53(2), 2012.
- [23] Alexander Kiselev and Changhui Tan. Global regularity for 1D Eulerian dynamics with singular interaction forces. *SIAM Journal on Mathematical Analysis*, 50(6):6208–6229, 2018.
- [24] Hailiang Liu and Eitan Tadmor. Spectral dynamics of the velocity gradient field in restricted flows. *Communications in mathematical physics*, 228(3):435–466, 2002.
- [25] Grégoire Loeper. Quasi-neutral limit of the Euler–Poisson and Euler–Monge–Ampère systems. *Communications in Partial Differential Equations*, 30(8):1141–1167, 2005.
- [26] Kunhui Luan, Changhui Tan, and Qiyu Wu. On the Euler–Poisson equations with variable background states and nonlocal velocity alignment. *arXiv preprint arXiv:2505.02992*, 2025.
- [27] Luca Natile and Giuseppe Savaré. A Wasserstein approach to the one-dimensional sticky particle system. *SIAM journal on mathematical analysis*, 41(4):1340–1365, 2009.
- [28] Olga S Rozanova. The repulsive Euler–Poisson equations with variable doping profile. *Physica D: Nonlinear Phenomena*, 472:134454, 2025.
- [29] Eitan Tadmor, Young-Pil Choi, Dong-ha Kim, and Dowan Koo. Large-time behavior of pressureless Euler–Poisson equations with background states. Available at SSRN 5358702, 2025.
- [30] Eitan Tadmor and Hailiang Liu. Critical thresholds in 2D restricted Euler–Poisson equations. *SIAM Journal on Applied Mathematics*, 63(6):1889–1910, 2003.
- [31] Eitan Tadmor and Changhui Tan. Critical threshold for global regularity of the Euler–Monge–Ampère system with radial symmetry. *SIAM Journal on Mathematical Analysis*, 54(4):4277–4296, 2022.
- [32] Eitan Tadmor and Dongming Wei. On the global regularity of subcritical Euler–Poisson equations with pressure. *Journal of the European Mathematical Society*, 10(3):757–769, 2008.
- [33] Changhui Tan. Eulerian dynamics in multidimensions with radial symmetry. *SIAM Journal on Mathematical Analysis*, 53(3):3040–3071, 2021.
- [34] Dongming Wei, Eitan Tadmor, and Hantaek Bae. Critical thresholds in multi-dimensional Euler–Poisson equations with radial symmetry. *Communications in Mathematical Sciences*, 10(1):75–86, 2012.

(Kunhui Luan)

DEPARTMENT OF MATHEMATICS, UNIVERSITY OF SOUTH CAROLINA, 1523 GREENE ST., COLUMBIA, SC 29208, USA

Email address: kunhui.luan@sc.edu